Impact of Photovoltaic Generators and Electric Vehicles on a weak Low Voltage Distribution Grid

by

Gudivada Venkata Thulasi Prasad

B.E., Anna University, 2010

A THESIS SUBMITTED IN PARTIAL FULFILLMENT OF THE REQUIREMENTS FOR THE DEGREE OF

MASTER OF APPLIED SCIENCE

in

The Faculty of Graduate Studies

(Electrical and Computer Engineering)

THE UNIVERSITY OF BRITISH COLUMBIA

(Vancouver)

December 2012

Abstract

In this thesis, the behaviour of a weak power distribution grid at the Point of Common Coupling (PCC) in the presence of a Photovoltaic (PV) inverter and Electric Vehicles (EV) as loads is analyzed. The grid connected to PV and EV has high impedance. The impact at PCC when the injected power varies in conjunction with the frequency and voltage deviation with a delay in inverter fed power is elaborated. Various measures such as peak shaving, coordinated charging, voltage drop correction have already been developed to mitigate the impact at PCC. These measures are observed on a combined EV and PV setup. In general, the grid tied inverter injects power based on an average grid voltage calculation at stable synchronization with the grid. If an error (for instance, an error in average grid voltage calculation) persists in such a case causing a loss in synchronization between the PV inverter and the grid, then a delay in the power injected may result in an oscillation at the PCC. A simple two bus system is considered to analyze the result of transportation delay. The delay and droop parameters of the PV inverter are altered whose results are quantitatively analyzed. The model abides the grid codes for active power reduction and static voltage support requirements. Further, the impact of a fault along with an inverter delay is analyzed. Simulative analysis is performed in the DIgSILENT PowerFactory software. To reduce the impact at PCC, performance criteria are analyzed whose parameters could be measured and altered. Scenarios are developed to analyze EV's impact in the presence and absence of storage and Distributed Generator (DG) that can be extended onto the micro grids.

Table of Contents

List of Figures

Abbreviations

AVR	Automatic Voltage Restorer
B	Susceptance
ECP	Electrical Coupling Point
EMS	Energy Management System
EV	Electric Vehicle
EVSE	Electric Vehicle Supply Equipment
EU	European Union
DER	Distributed Energy Resources
DIgSILENT	Digital SImuLator for Electrical NeTwork
DPL	DIgSILENT Programming Language
DSL	DIgSILENT Simulation Language
DSO	Distribution System Operator
G	Conductance
GC	Grid Code
GTI	Grid Tied Inverter
LV	Low Voltage
MG	Micro Grid
MPP	Maximum Power Point
P	Active Power
PCC	Point of Common Coupling
PDG	Power Distribution Grid
PI Controller	Proportional-Integral Controller
PLL	Phase Locked Loop
PV	PhotoVoltaic
Q	Reactive Power
SOC	State Of Charge
SCC	Short Circuit Capacity
SCR	Short Circuit Ratio
STC	Standard Temperature Conditions
U (or) V	Voltage
VSC	Voltage Source Converter
V2G	Vehicle to Grid
X	Reactance
Z	Impedance

Acknowledgements

My First and foremost humble gratification to the love and blessings of my parents. I whole heartily thank Professor William Dunford, for his guidance, encouragement and support throughout my graduate studies.

I thank the Power Electronics department of Siemens Corporate Technology for giving me an opportunity to work on my master thesis in Germany. Sincere thanks to Dr. Mathias Duckheim, Mr. Thomas Lehmann, Dr. Johannes Reinschke, Dr. Dominic Buchstaller and Dr. Sasidharan Sreedharan for their valuable guidance from the very early stages of my work. Your support and encouragement has provided clarity to my research work.

I would also like to acknowledge Dr. Jayakrishnan R. Pillai, Ioannis Theologitis, Mrigank Sharma, Hamid Atighechi and Darvesh Abbas for their expertise, advice on using the software tools and discussions in relevance to my study for this project. I thank my friends and colleagues at the University of British Columbia and Erlangen for their moral support and encouragement.

To my Parents

1 Introduction

The energy demand in the coming decade is projected to double due to a continuous population growth [1]. Improvement in energy efficiency of current technologies along with renewable energy sources integration is seen to feasibly answer this energy demand. With a focus toward Renewable energy grid integration, countries such as Germany, Spain and USA have improved their legislation framework to promote the same. Several countries have shown dedicated research through dynamic and stability analysis due to the increase in grid tied systems. Through the changes happening toward a renewable environment, new problems have risen. The integration of a substantial share of decentralized generators into a conventional grid which wasn't designed for this purpose could create instability issues to the grid. The increase in PV must be compensated with new dynamic compensation solutions that independently allow the conventional active power trade between PV and utility. This also includes measures such as voltage control, power oscillation damping, power factor correction and harmonic filtering. These measures are expected to be more predominant in the near future due to the increase of not just the renewable penetration, but also due to the projected market growth of EV sales. Many countries worldwide have set several aggressive targets for the wide spread use and adoption of the EVs. Figure 1 shows the national sales targets set by various countries for EVs by the year 2020 [2].

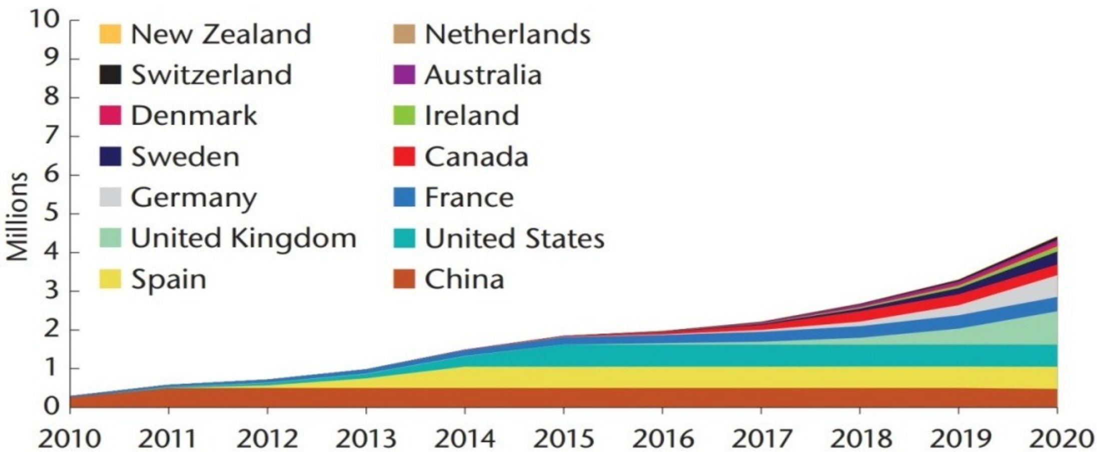

Figure 1 National EV sales targets, 2010-2020 [2]

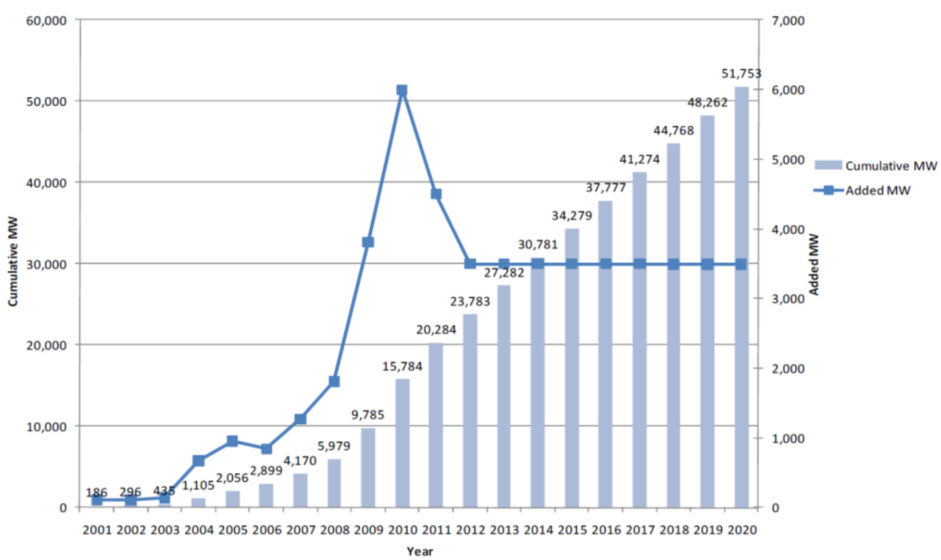

Figure 2 Increase in renewable energy sources in Germany [3]

Similarly significant analysis for PV grid connected systems can be obtained through information from German National Renewable Energy Action Plan (NREAP). It is seen that since 2004, Germany in particular has seen a huge growth in PV installations. This is mainly due to the feed-in tariff policy mechanism and relevant subsidies that have been in effect. It is evident from Figure 2 that from 2008, Germany's renewable power has been tracking a huge increase until now.

Impact of PV and EV on a weak grid

The rigidity of a grid is determined based on the short circuit power ratio. This is a ratio of apparent short circuit power to the maximum apparent power at the PCC where PV and EV are connected. A detailed explanation of the ratio in a weak grid will be discussed in later chapters. In a weak grid, the voltage level is not constant as compared to a normal grid [4]. The voltage values and fluctuations in a weak grid must be taken into account because of its higher probability to exceed the standard limits. The grid impedance is significant and has to be considered in order to have valid conclusions. A normal grid designed for relatively small loads, turns into a weak grid due to an addition of large electric loads that increase the impedance of a grid. The summation of impedance of the line, transformer and other circuit components add to the total impedance at PCC. The loads add to this impedance and hence the presence of EV (larger loads) might increase the impedance at the PCC. A grid can be characterized either weak or strong by different parameters. In addition to its voltage level and its total power capability, the short circuit capacity (SCC) can be defined which is mainly dependent on the rated voltage and the absolute value of impedance of the grid that can be measured at this point. Hence, it is possible that the additional loads might turn the grid weak. The grid impedance is the sum of all the grid components which might differ from region to region. It consists of the impedance of the transmission line, which mainly depend on material, diameter and length of the line. Further this grid, limits the PV power that can be injected into it after reaching a certain limit. The reason is that the additional loads add to the high impedance leading to a voltage level below the minimum limit. This can be related with the PV nose curve characteristics. Here, the thermal limits are exceeded and no further power can be absorbed by the grid. In such a case, an increase in the penetration of PV power at PCC might lead to voltage violations. Further if the PV inverter loses synchronism with the grid due to an error, it might cause an unexpected delay in power injection leading to oscillations at PCC. In a MG with rated active loads and renewable sources, the Short Circuit Raio (SCR) at the PCC is defined as (2.1) [5].

$$SCR = \frac{V_{Grid}^2}{Z_{weak} S_{rated}} \tag{2.1}$$

Aim and objectives of thesis

This thesis analyzes the impact of PV penetration and EV loads in a distribution network. The investigation is extended through a simulative analysis, abiding the grid codes, to study the impacts of EV and PV at the grid.

- A Review over the existing EV charging strategies and measures to dampen its impact on the Power Distribution Grid (PDG).
- Simulative analysis of
    - Interaction between an inverter controller and the network,
    - Steady state active power reduction, voltage support and analysis during fault.

Study purpose

The reason for this study is to learn about the potential impacts that may arise due to high EV and PV penetration. The study will include a mixture of both of these elements in power system under different scenarios. Analysis of a few performance criteria and measures to reduce the combined electrical impact at the PCC is a part of the study. In general, for systems which are in the planning stage, similar to the research in this thesis, typical models and parameters are created for an initial study. Hence a simple model's operational problems are analyzed in a simulative environment. An analytical study of the simple grid includes steady state and faulted condition analysis. A detailed modeling of the relevant components is presented. It is expected that these results would support the industry partner's project goals.

Advantages of EV and PV integration in the power grid

The main reasons for integrating EVSE into the power grid are that the EV is pollution free at the point of use, provides freedom for consumers to choose their own charging time, charging rate and the ability of V2G power flow for grid stabilization. Due to the charging time and evening peak load overlap [7][14], strategies must be initiated to mitigate its impact.

A control through an Energy Management System (EMS) at the PCC where the EV and PV are connected can alter the power flow to the battery. When power production through PV is higher, through the control one can shift this power to match the peak load demand time. The possibility of utilizing the EVs as a storage medium and exchange with grid is advantageous. This opportunity to level out the demand during day (for example when PV production is high) to evening load demand can be efficiently met. Further, EVs in society would help reduce air pollution compared to conventional vehicles. An efficiency of the EV conversion is about 59-62% of electrical energy from the grid to power its wheels, compared to a gasoline car which converts typically 17-21% of energy stored in gasoline to power its wheels [8]. All these features allow EV as battery storage to stand out and importantly counter the fluctuations caused due to PV production to help balance the entire system.

Extending the objective to a simple model and a case study

In a power system network consisting rotating generators, frequency droop control is one of the ways to stabilize the grid based on the mechanical inertia of the generating turbine. In case of static generators like PV inverter, similar control strategies can be implemented. The two control loops, frequency control which controls active power and the voltage control loop which controls reactive power injected into grid are the basis of any power system network control. One of the methods is droop control, which injects the active power as a function of frequency change, P (Δf) and reactive power as a function of voltage change, Q(Δu). This control is studied here on a simple model to relate the power injected into the grid. The simple two bus system consists of an inverter rated 0.5MW and load rated 0.25MW. Also, the active power reduction and reactive power for voltage support features are studied. Controllers are designed for a specific model. However, the actual system differs from the model, leading to imperfections in the control strategy. In this context, we study a delay in the power injected at the PCC. The delay results a low voltage and low frequency fluctuation of ranges (for example, 5 to 10 Hz) at the PCC which are analyzed. The delay in synchronization is expected to be one of the potential impacts caused by a PV grid tie inverter. Electric Vehicles considered as loads in such a weak residential grid are expected to worsen this impact. Some case scenarios are summed up as an extension to the analysis over simple model studied in DIgSILENT PowerFactory software.

Thesis Outline

This thesis consists of six main sections. Section 2 discusses an overall view about the PV and EV grid connected system. This includes discussion about the expected impacts on the present PDG in the vicinity of EV and PV penetration. Performance criteria formulated along with measures to mitigate the impact in general are discussed here. The Literature overview includes considerable factors involved before implementing the system in a real time.

Section 3 elaborates the theory behind the control of frequency and voltage through power injection at the PCC. This section discusses the droop control and introduces the basic norms of the German Grid Codes.

Section 4 describes a simple model in its equivalent state space representation through analysis of its equivalent circuit.

Section 5 describes an outline of the simple model in a simulative environment. The simple model with 0.5 MVA capacity built by DIgSILENT is elaborated. The details include description over the blocks and slots used in the software tool. This section further includes the steady state analysis for active power reduction and voltage restoration through reactive power support. This section also analysis the model during fault conditions. The system's ability when being used as a generic model for PV systems must comply with the grid codes. The system is investigated with reference to the German GC. The results are quantitatively analyzed through curve fitting in MS Excel. Finally, the possible extension of the simple model to a network case study with real time data is analyzed and documented.

Section 6 provides literature of previous research work pursued particularly with respect to the charging strategies of an EV grid tied system. The conclusions include potential future work of this project and a summary of the thesis. The appendix section details the characteristic of the model used. It covers in depth details of the model including simulation language codes and a few other parameters of the model.

2 Current Scenario, Performance Criteria and Measures

In this chapter, a study of the current distribution system that is designed typically for a specific load carrying capability purely based on daily load consumption patterns is analyzed. When EVSE is deployed in such a system, the electric power demand patterns change due to the added load. Moreover, fast charging of EVs delivers high energy transfer that results in voltage flicker at the PCC [9]. Over the past few years, there has been a concern at the PDG with respect to the renewable penetration. This chapter analyzes the potential impacts on a grid tied PV inverter with an EV at the PCC. Possible remedies are explored and corresponding measures to mitigate the impact are formulated in reference to the listed performance criteria.

2.1 Current Scenario and Problems

As mentioned earlier, the present PDG can handle only a specific capacity of load, considering the daily load distribution at the consumer end. Sudden inclusion of EV loads is expected to impact the PDG's characteristics. There are several problems discussed in research articles and reports, of which a few issues are listed below.

- *Violating Voltage limit:* Voltage drop or rise also termed as swell and sag respectively at the PCC may be due to fast charging stations for electrical vehicles [9]. The energy consumption may vary significantly due to the stochastic nature of uncontrolled EV charging leading to voltage violation at PCC.
    - The standard BS EN 50160 on "Voltage characteristics of electricity supplied by public distribution systems" (cf.[11]. p.3), provides limits and tolerances for various phenomena occurring at the PCC.
    - The addition of DERs along with uncontrolled EVs charging may cause voltage fluctuations in the LV network [12]. In particular, higher DER power injection could lead to overvoltage problems in LV networks. Generally accepted standards expect the voltage to be between 95 % and 105 % of the base network voltage.

- *Voltage flicker:* The randomness or fluctuation in loads such as EV and sources such as PV, may lead to a pulsating load causing a variation of the voltage with a sufficient duration known as flicker. Voltage flicker may also be caused by inter-harmonics emitted by power electronic interfaces used for connecting EV and PV units. It might cause additional voltage peaks at the LV distribution transformers, adjacent cable systems, PCC & other power distribution components [13 pg. 72].

- *Frequency Variation:* In micro-grids and islanded systems, frequency variations can occur by the connection of a large number of EVs at the same time.
    - If EV load demand (due to large number of EVs at the same time) is not matched or compensated through increase in power generation, it might lead to variations in frequency at the grid level. EN 50160 defines a certain limits from the supplier's point of view for interconnected and non-interconnected systems and IEC 61000-2-2 defines emission and immunity levels for equipment connected in LV networks (cf.[13]. p. 71).

- *Over Loading:* (eg., Cable and Transformer Loading):
    - Overloading can be subcategorized into long term and short term. The former referring to thermal overload for example on distribution lines, transformers and other components. The latter can be referred to overloading at the PCC especially during peak load time due to additional EV loads along with conventional loads.
    - It is expected that particularly the EV loads, would tend to increase the threshold value of the transformer to be overloaded [14]. The threshold value is chosen to be 1.16 for a transformer instead of 1, so that the standard transformer can withstand instantaneous peaks without a problem. The transformer overloading is found to be larger in case of an uncontrolled EV charging as explained in the appendix. Also, its thermal overload conditions are elaborately discussed in (cf.[15]. p. 5-26).

- Power flow at the PCC: The active power consumed at PCC exceeds the limits due to the two EV and PV. Also the power factor at PCC is to be corrected through measures.

- Power factor exceeds the DSO limits mainly due to uncontrolled charging of EVs.
- Quarter-hour energy limit (at the PCC): This relates to either excess of power flowing at PCC due to EV charging or another condition where the quarter-hour energy limits are not used to their fullest potential. Appropriate load scheduling, load shifting and usage of storage devices would be possible remedies here.
- Further, the low average line capacity usage is an additional constraint that is seen to exceed the limits and also seen to be used lesser than its potential which requires measures for load scheduling and controlled charging strategies.

The above mentioned points are in close relation to each other. It could be understood that the main problem in the present grid at the PCC is particularly due to the EV charging pattern and PV power penetration into the grid. The next sections elaborate the characteristics of PV and EV tied to the grid.

2.2 **Photovoltaic Generator and Electric Vehicle Grid Integration**

This section provides basic factors and characteristics for analysing the impact of PV and EV on the PDG. This is followed by a list of performance criteria and measures to influence and mitigate the impact at PCC.

2.2.1 Photovoltaic Impact and Advantage

Figure 3 provides three conditions in case of the system connected to grid. The explanation includes power consumed at the local load, P_L at the PCC. P_{AC} is the active power flow and Q is the reactive power flow at PCC to the grid. P is the active power that is injected at the point on the generator side.

$$P_L = P - P_{AC} \tag{2.1}$$

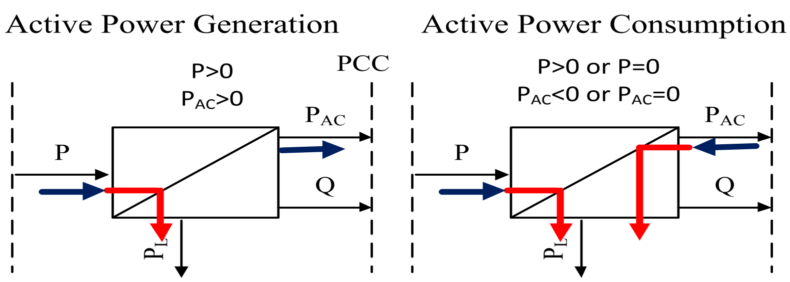

Figure 3 Power flow at the PCC seen in the grid coupling converter [16]

During the condition when generator active power P is larger than the self-consumption (ie., when $P_{AC} > 0$, power is fed into the grid). Here, the power from photovoltaic unit compensates all losses. In another condition, when $P < P_L$, then additional losses prevail, power is absorbed from the grid and not fed into the grid ie., $P_{AC} < 0$. In the third condition, when $P = 0$, the standby losses have to be compensated by the active power from grid, resulting in $P_L = - P_{AC}$. Consideration of these conditions is necessary as the costs of energy losses compensated by the grid may be different when compared to the compensation by photovoltaic active power [16].

There are several advantages of renewable energy over conventional power generation (cf.[1].p.9). However, there are also considerable impacts. The following section explains these aspects.

2.2.1.1 Size and Location of PV

The impact of PV installed at various locations along with changes in its penetration levels has been seen to increase the voltage level. The research article [17] provides an insight through case studies showing PV with various penetration levels at different sites. It shows a variation size of 1 to 1692 kW that increases system voltage level up to 0.2%. The same research concludes that the best location for placing a PV inverter would be at the end of the line. The reason is that, the occurrence of a fault in any part of the line can be isolated before reflecting onto the customer end. PV serves as the downstream side for customers so that the number of outages can be reduced.

2.2.1.2 PV inverter to improve the voltage profile

The ability of a PV inverter to inject real and reactive power stands as an important feature that is discussed in a simulative environment in this thesis. However in an unbalanced three-phase PDG, injecting real power from PV in any one phase deteriorates the voltage profile in the other two phases (cf.[17]. p. 88). This is a result of mutual impedance between phases.

PV can influence in correcting losses and power factor of PDG. The research paper [18] discusses a possibility of reducing loss based on a power summation method.

2.2.1.3 Reliability analysis of the PV generator

While the system is in the stage of planning and analysis of operating conditions, calculation of its reliability through indices is helpful. It fosters uniformity in the development of distribution service in identifying the factors that affect the indices. Such analysis aid in reporting practices amongst utilities. (cf.[19].p.1). The calculation of indices for a PV grid connected generator is recommended as a measure of the reliability of the system. The IEEE guide for reliability indices presents its terms and definitions which are used as a base analysis in many research papers. Research work in [20] defines the reliability indices practices in US and also discusses outage factors and roles in reliability calculation. Along with these reliability analyses for planning and operating conditions, a few performance criteria that can be influenced and measured are described in the later sections.

2.2.2 Electric Vehicle impact and Characteristic

This section explains the EV charging strategies and general characteristics. The EV is seen as a potential that can provide two main functions namely grid-to-vehicle (G2V) and vehicle-to-grid (V2G) power flow. There is a plenty of research focussing on measures to resolve EV grid penetration impact [31][38]. The reason for this interest is that the EV control is flexible compared to a household load. Flexibility includes its characteristic that can act as both, a load as well as a source. Determining a curve based on EV fleet charging or discharging is less accurate as there is a very little historical data. Therefore a single EV profile needs to be acquired based on which the fleet behaviour can be modeled with its corresponding “plug-in” time. Several EVs charging at the same period of time will increase the power demand on the grid as a function of voltage and amperage.

2.2.2.1 Charging characteristics

Duvall et. al., [21] discusses several options for connection EV to the grid. A comparison over charging time period as an example for three major EV categories (based on battery size) is provided in Table 1. EV with larger battery sizes require more charging time. The discussions include the EV charging analysis based on the voltage and amperage values. At 120 volts AC, a 15 amp circuit can charge a 1.4 kW load, a 20 amp circuit can charge a 2 kW load. A 30 amp circuit can charge as much as a 6kW load at 208 or 240 volt AC supply.

PHEV - 20	Battery size	Charging circuit	Charging time
Compact Sedan	5.1 kWh	120 V_{AC}/15 A	3.9 to 5.4 hrs
Mid-size Sedan	5.9 kWh	120 V_{AC}/15 A	4.4 to 5.9 hrs
Mid-size SUV	7.7 kWh	120 V_{AC}/15 A	5.4 to 7.1 hrs
Full-size SUV	9.3 kWh	120 V_{AC}/15 A	6.3 to 8.2 hrs

Table 1 Time required for charging PHEV – 20 from 20% SOC to 100% SOC

2.2.2.2 Plug in time of EV

This is another important criterion. The optimum time for charging EVs, from utilities point of view could be varied for true optimization. In general, the power demand in the nights is low. From consumer's point of view, it is a comfort based preference, i.e., easy access to charge ones vehicle is during the evening hours (after return to home from work). One of the analyses shown in the ORNL report [22] uses a weighted average charging profile that calculates a rough aggregation. The number of EVs on road is multiplied with the hourly demand from the load curve for each region to calculate the hourly addition to the system electrical load. The article calculates weighted average values with a few assumptions. It broadly classifies the charging period to evening charge and night charge periods. During the evening it is assumed that half the number of vehicles are plugged in at 5pm and the other half at 6pm. During the night, a half of the EVs are plugged in at 10pm and another half at 11pm. The vehicles remain plugged in until they are fully charged. A weighted average profile as a result of two assumptions is shown in Figure 4 (cf.[22].p.9).

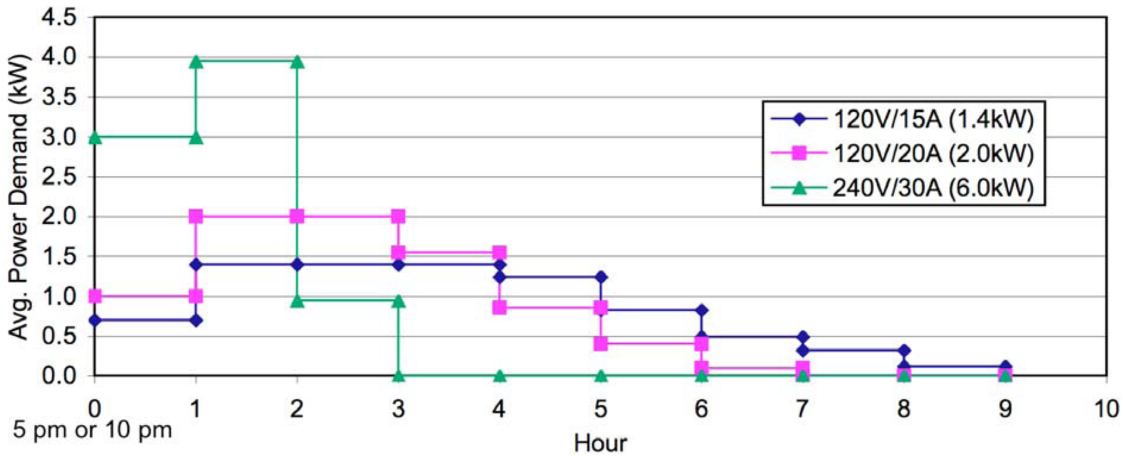

Figure 4 The resulting weighted average charging profile

The utilities try to modify customer choices through pricing schemes (favouring night time charging), regulations and incentives. There are some features where the charger itself intelligently decides when and how much to charge based on SOC and charging rates [23].

The FERC's National Action Plan on Demand Response [10] has identified the study of how plug-in hybrid electric vehicles interact with demand response. Most of the research on EV penetration into the power system is based on fixed charge profiles which are not controllable. Though there have been different assumptions such as evening charge or off-peak charge, EV charge time is still in lack of flexibility. EV charge time and charge rate should be flexible for a realistic study. There is a need to perform analysis of EV penetration into the distribution network and the interaction with existing loads. In one possible scenario, the EV can be considered as one of the household loads and included in the appliance list that can perform demand response. In this thesis, the former alone is considered. ie., EVs are seen as mere loads. However it is essential to consider the V2G characteristics to have a detailed analysis of the EV support at LV grid.

2.2.2.3 EV deployment in PDG

The extent to which the EVs are deployable in a PDG must be strategically planned. This again depends on the charging power level and charging time. The different charging levels and the time it takes to charge EV is listed in the Table 2. The fast chargers deliver energy in a short time interval but their high charging power result in pulsating loads that leads to voltage flicker affecting grid and transformer loading [9].

Charging Level	Voltage (Volts)	Current (Amps)	Power (kW)
AC Level 1	120	12 - 16	1.44 – 1.92
AC Level 2	208 - 240	12 - 80	2.5 – 19.2
DC Level 1	200-450V	<=80A	<=19.2KW
DC Level 2	200-450V	<=200A	<=90KW
DC Level 3 (fast charging)	200 – 600 V DC	250, 350, 400 A	<=240 kW

Table 2 Electrical rating for charging levels (cf. [15]. Section 5)

2.2.2.4 Impact of Electric Vehicles

Potential threats are one of the reasons for research on grid connected EV systems. When the EVs are considered to charge in an uncoordinated manner, the impact measured in terms of penetration (or seen as accumulation of large loads) is beyond a certain percentage of allowed levels. The research article (cf.[23]. sec 3.5) shows an average and extreme values of voltage deviations, and power losses in case of an uncontrolled hybrid electric vehicle charge with a penetration of 30%. In the case (considering extreme values), the power losses without EV charge at the grid is 1.7% whereas uncoordinated charging leads to double the power loss equal to 3.5%. The literature review in the following section discusses some methods to establish a charging scheme that reduces the impact of Electric Vehicles on the PDG.

2.2.2.5 Economic Potential Advantage of EV integration

EVs bring many potential benefits to the power system. One of the most significant contributions is that their higher adoption will bring higher revenues for utilities. The research in (cf.[25]. sec. 2.2.2.3) refers to data from EIA for average electricity price and elaborates the use of EV's economical potential. An average retail electricity price is 11.36 ¢/kWh. A typical PHEV-20 with battery capacity of 6kWh on a daily charge can bring about $250 per annum of additional revenues for every single EV in service. Considering a penetration of 1% EV into the market in 2015 (conservative estimation from Morgan Stanley's report of penetration), sums to revenues worth 62.5 million dollars per year.

2.3 **Performance Criteria**

A list of problems discussed in section 2.1 can be measured and corrected through a few alterations in parameters, for which their performance criteria must be analyzed. For instance, a simple model can be assessed with criteria that can control the supply-demand mismatch, component overloading, etc... These parameters, when altered, can yield significant improvements for the grid tied system.

This section lists a few performance criteria with which possible solutions and measures can be traced to address the electrical impact at PCC.

- Amount of Self-consumption
  - Self-consumption means production and consumption of power in the same location. It is significant because it avoids power transmission & conversion loss.
  - Electricity prices and incentives in several countries, including Germany are focused on self-consumption to lessen the burden on power grids.
  - It encourages consumer's interest toward energy conservation.
  - Ideally the consumption matches generation, eg, if the PV power injected equals to the power consumed in the house. This is also referred to as matching and increases the prosumer characteristics (Prosumer is Producer + Consumer).
  - We define the Self consumption index as,

$$SC = \frac{P_t - P_f}{P_t} \tag{2.2}$$

SC - is defined as the self-consumption index
P_t - is the total power produced and
P_f - is the power fed into the grid

- Amount of energy unused (peak power which would be wasted otherwise)
  - If the PV power produced is not used to the fullest extent, it is considered as wastage. So measures must be taken to use the peak PV power production to the fullest extent.
  - To quantify, the amount of PV generation exceeding the load demand, particularly in the peak power production time is formulated.
  - A generalized form of unused energy with EV load is given in the following equation.

$$E_{wasted} = \int_{t=t_1}^{t_2} \left(P_{PV}(t) - P_l(t)\right) \text{ where } x = P_{PV}(t) > P_l(t); \left\{x \in R \mid t_1 < x < t_2\right\} \tag{2.3}$$

$$P_{car}(t) = n_{EV}(t) P_{EV}(t)$$

$$P_l(t) = P_{car}(t) + P_f(t)$$

E_{wasted} - is the amount of unused energy;

$P_l(t)$ - is the power consumed by loads at time t;

$P_{PV}(t)$ - is the power produced by photovoltaic cells at time t;

$P_{car}(t)$ - is total power consumed to charge EV's at time t;

$n_{EV}(t)$ - is average number of EV's charged at time t;

$P_{EV}(t)$ - is the average power consumed by a single EV at time t;

$P_f(t)$ - is power fed into grid in time t.

- Analyzing grid capacity
    - To improve the system efficiency, it is necessary to analyze the grid capacity so that measures can be taken to reduce the amount of unused line capacity. The available grid capacity can be improved through storage and/or load management [26]. The amount of power that the utility can distribute over an MV line is limited (based on voltage and thermal limits) which is further hindered by fluctuations in EV & PV power injection. Research paper [27] shows the potential to transfer extra energy within the capacity of an existing grid
    - By smoothing the peaks, line capacity is restored to its best efficiency (eg, storage). The examined capacity was made available by matching storage and flexible load management methods with supply and demand.
    - Research paper [26] examines the part of the capacity which is needed to supply the peak demand. This part is only partially used because the demand fluctuates over time. Measurement of the line capacity is shown below. $P_{average}$ is shown as the dotted line and P_{load} is the continuous line shown in Figure 5.

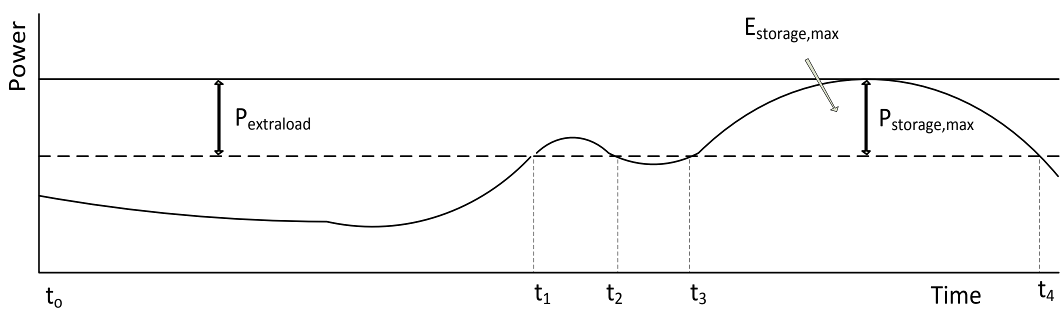

Figure 5 Levelling the load with storage

$$P_{\text{avg}} = \frac{1}{T}\int_{0}^{T} P_l(t)dt$$

$$P_{storage,\max} = \max\left|(P_{avg} - P_l(t)\right| \quad \textit{When, } t \in \{P_l(t) > P_{avg}\}$$

$$E_{storage\max} = \max_{i=0\ldots n} \left| \int_{t_1}^{t_{t+1}} \left(P_{avg} - P_l(t) \right) dt \right| \tag{2.4}$$

Where, T *is the total time*;

P_1 *is the power of the load and* n *is the number of times the* P_1 *is equal to* P_{avg};

$P_{\text{Storage,max}}$ *is the power stored and* $E_{\text{Storage,max}}$ *is the energy capacity of storage*;

n *is total number of times when* P_1 *is equal to* P_{avg}.

- The amount of loads that is supplied by distribution grid can vary with time. In such a condition, an additional extra load in peak demand period may not be met with power generation. This situation is opposite during off peak periods. Hence, the non-critical loads may have to be managed over time through load management. P_{peak} is the peak power over time, P_{load} is the regular load and $P_{\text{extraload}}$ is determined as shown below,

$$P_{extraload}(t) = P_{peak}(t) - P_{load}(t) \tag{2.5}$$

2.4 Possible Methods to Mitigate Impact at Grid Connection Point

Below is a list of methods that can mitigate the impact at grid connection point.

- Voltage drop correction:
  - Voltage drop can be corrected through the use of voltage regulating equipment (cf.[27] .p.758). Voltage-regulating equipment is designed to maintain a predetermined level of voltage automatically that would otherwise vary with the load. As the load increases, the regulating equipment boosts the voltage at the substation to compensate an increase in voltage drop at the distribution feeder.
  - Tap changing method for line voltage regulation (cf.[27]. p. 758) [28]: Taps are connections on a transformer winding through which the turn's ratio can be altered. Motor-driven automatic tap changers are necessary for voltage regulation with widely fluctuating loads (EVs). This is called Tap Changing Under Load (TCUL) or load tap

changing (LTC). LTC is us ed in distribution substations to keep the secondary line voltage at the proper level in response to load and primary voltage changes.

- Regulating transformers are designed to provide a boost in voltage magnitude along a line or a change in phase (cf.[27]. p. 758).
- Use of Capacitors: Most loads are lagging or inductive in nature. The line reactance is much greater than the line resistance. Switching shunt capacitors across a line will increase the voltage by reducing the inductive VARs drawn by line (cf.[27]. p. 758).

- EV control based on the micro grid (MG) frequency and voltage:
    - One possibility to mitigate EV impact is by reducing the power drawn from the grid with respect to the system frequency through droop control strategy and Load frequency Control (LFC).
    - The frequency and voltage are an instantaneous indication for the power balance in the MG. It can be used to adapt the active power charging of the EV batteries and the amount of reactive power that is required from a PV inverter. For this purpose, a control approach, droop-controlled inverters was developed and elaborated (cf.[30]. p. I-133). This is done by reducing the power transacted between the grid, loads and PV with respect to the power system frequency and voltage.
    - Voltage drop in a distribution feeder can be corrected by applying voltage regulating equipment (cf.[27].p. 758), which is designed to maintain a predetermined level of voltage automatically. Without voltage regulating equipment, the level of voltage would vary with the load. As the load increases, the regulating equipment boosts the voltage at the substation or transformer station to compensate for the increased voltage drop in the distribution feeder. The influence and relation between voltage and frequency with respect to power at PCC is explained in the Chapter 3.

      Examples of voltage-regulating equipment are:

        - Tap changing or regulating transformers,
        - Use of capacitors or use of inverters with actively controlled power factor.

- Coordinated charging:
  - Controlled charge of EV (as a function of the voltage at the node where cars are connected) allows to charge an important number of cars within an acceptable period avoiding overloads of grid tied components. Uniformly distributing the charging of EVs to off-peak time is referred to as uniform coordinated charging (cf.[31]. p. 104 – 105). The permissible charging power is a function of the nodal voltage at which the EVs are connected. Controlled charging of EVs, allow charging of a significant number of cars within an acceptable period avoiding unacceptable voltage drops.
  - Staggering the PHEV charging time: In the study [7], the stagger charge implies that the EVs are allowed to be charged only when the current load (kW) seen by the distribution transformer is less than a specified value, i.e. when the current distribution transformer load does not exceed its original peak load.

- Power factor correction: A compensation device such as a Static VAR Compensator (SVC) may be used for power factor correction. An SVC is capable of providing reactive power within a very short period of time. The SVC is an automated impedance matching device, designed to bring the system closer to unity power factor, regulate the voltage and stabilize the system. SVC is installed to reduce voltage flicker in industries [32].

- Load shifting:
  - A supply-demand mismatch can be eliminated or mitigated by means of storage devices (e.g. stationary batteries) and coordinated supply to meet demand with storage operation through an appropriate energy management. This notion is often referred to as "load shifting" i.e., a service which can be shifted to another time where demand is low or supply is high. This is feasible using storage (long term and short term). (For eg, Load shifting of the PV energy from day - to night using storage system). Batteries, flywheels, super conducting magnetic storage system and thermal storage like ice storage can also be implemented.
  - As the last condition, when all storage elements are completely used, dump loads might help to smooth the power fluctuation. A dump load is an electrical resistance heater that

must be sized to handle the full generating capacity. Dump loads can be air or water heaters, and are activated by the charge controller whenever the batteries or the grid cannot accept the PV energy being produced. Excess energy is "shunted" to the dump load when necessary to a useful form (eg., using water heating tanks) [33].

- Demand response (consumer/grid based):
  - Demand response program shifts load by controlling the functions like air conditioners, refrigerators, water heaters, heat pumps, and similar electric loads (deferrable loads) to satisfy demand period.
  - The interaction between consumer & utility in a system is important as it allows control from service provider during emergency.
  - In interactive dispatch control, the utility can command an inverter, e.g. to ride through voltage sag. Interactive control will also enable the distribution system to direct the inverter to go off-line when there is a fault, rather than relying on multiple inverters, each supplying power to the grid, to independently detect a fault.

2.4.1 Measures in equivalent cost factors with performance criteria.

When any specific parameter is outside its specified limits at the PCC, it can be measured by considering the violation of the limits specified by the DSO. The violation (in case of voltage as an example) can be measured using different norms, such as

1. The total number of occurrences of voltage limit violations,
2. The magnitude of overvoltage or undervoltage, by which the limit is exceeded.
3. The maximum overvoltage or undervoltage for all voltage limits violations.

- <u>Measure – Voltage Violation</u>: The different violations of voltage limits at the PCC can be measured by the subsequent formula, which encompasses all of the three afore-mentioned criteria. The value of the violation can be associated with a suitable cost factor, if available. Otherwise the cost factor is 1 or 0, when the corresponding norm is not considered.

$$C_t = C_N N + C_v \Delta V + C_M M \tag{2.6}$$

C_t *- the total cost function*

C_N *- cost factor corresponding to* N

N *- total number of times the limit is violated*

C_V *- the cost factor corresponding to* ΔV

ΔV *- the total amount of voltage deviation exceeding the limits*

C_M *- the cost factor corresponding to* M

M *- Maximum amount of voltage amongst all violations*

A measure in this section is termed in reference to measuring the performance criteria which is essential for the research problem in-order to mitigate its impact. A few measures may involve statistical analysis ie., to collect the historical data and few measures require deterministic approach where values are determined.

Performance Criteria: The performance of any energy management system can be measured by evaluating the cost function with respect to their individual parameter at the PCC. This performance can be used under different scenarios to develop and support EV charging with DER and storage. Independently the values of the cost factors and the cost function needs to be reduced to improve the performance.

1. For $C_V = C_M = 0$ and $C_N = 1$, a reduction in the cost function corresponds to a reduction of the number of limit violations.
2. For $C_N = C_M = 0$ and $C_V = 1$, a reduction of the cost function corresponds to a reduction of the total amount of voltage exceeding limits.
3. For $C_N = C_V = 0$ and $C_M = 1$, a reduction of the cost function corresponds to a reduction of the maximum voltage violation.

- Measure – Quarter hour energy limit (at PCC) exceeding or not fully used: This relates to the typical energy supply contracts that contain a limit for the energy supplied within one quarter of an hour. If the corresponding limit is exceeded, high penalty costs have to be paid. As a consequence, violations of the quarter hour energy limit as specified in a typical supply contract have to be avoided. Lower limits for the amount of energy supplied within a quarter of an hour might be one of the specifications in the contract. Depending on the structure of the energy supply contract, a common cost function can be specified analogous to voltage violation. All the cost functions refer to the energy demand at PCC.

$$C_t = C_N N + C_P \Delta P + C_M M \tag{2.7}$$

C_t *- the total cost function*

C_N *- cost factor corresponding to* N

N *- total number, where peak energy demand exceeds energy limits*

C_P *- the cost factor corresponding to* ΔP

ΔP *- the total amount of energy exceeding energy limits*

C_M *- the cost factor corresponding to* M

M *- the maximal peak energy demand exceeding energy limits*

Performance Criteria: The performance of an energy management system can be measured by evaluating the cost function (2.7) with respect to the energy demand required at the PCC within each one quarter hour time interval. Independently of the values of the cost factors, the value of the cost function needs to be reduced to improve the performance. See also Subsection of voltage violation in the previous section for further explanation.

- Measure – Power Factor: The power factor (PF) is the ratio of the active power in (W) to the total power (active and reactive power) measured in the unit (VA).
    - The total penalty cost is a result of the large power fluctuation that violates certain DSO specified spectrum limits.

$$C_t = C_a N_1 + C_b \Delta E + C_c Q \tag{2.8}$$

C_t *- is the total cost;* C_a *is the cost factor corresponding to* N_1 *specified by DSO*

N_1 *- Number of times, the energy at PCC violates the quarter hour energy limits stipulated by DSO*

C_b *- is the cost factor corresponding to* ΔE *specified by DSO*

ΔE *- is the amount of energy above maximal threshold*

C_c *- is the cost factor corresponding to* Q *specified by DSO*

Q *- is the maximum amount of energy amongst all deviations from specified limits*

Note: During calculation, two out of the three cost parameters will be equal to zero

- Harmonic content out of specified limits
  - The total penalty cost is a result of the Harmonics out of spectrum or violation caused for operating beyond certain DSO specified limits.

$$C_t = C_l N_3 + C_m \Delta H + C_n H_m \tag{2.9}$$

C_t *- is total cost,* C_l *is the cost factor corresponding to* N_3 *specified by DSO*

N_3 *- Number of spectrum harmonics that exceed maximal spectrum DSO limit*

C_m *- is the cost factor corresponding to* ΔH *specified by DSO*

ΔH *- is the amount of spectrum frequency out of the specified spectrum limit*

C_n *- is the cost factor corresponding to* H_m *specified by DSO*

H_m *- Maximum frequency spectrum violation*

- Low average line capacity usage or untapped line capacity: The resulting cost incurred by the consumer due to improper utilization of the line capacity with reference to the explanation in the first paragraph under the section 2.4.1 is noted for line capacity here. This increases the capital cost, however improves the efficiency.

$$C_t = C_i N_4 + C_j \Delta V + C_k M \tag{2.10}$$

C_t *- is total cost,* C_x *is the cost factor corresponding to* N_4 *specified by DSO*

N_4 *- is total number of spectrum violation exceeding the DSO stipulated limits*

C_j *- is the cost factor corresponding to* ΔV *specified by DSO*

ΔV *- is the amount of spectrum voltage out of the specified spectrum limit*

C_k *- is the cost factor corresponding to* M *specified by DSO*

M - *Maximum voltage magnitude violation*

- EV driving pattern and SOC values
    - The EV Driving pattern directly influences EV penetration as the number of workers returning home to charge their EV, add as loads to the regular peak demand period. The driving profile follows a similar pattern which is summarized in Table 3 (cf.[35].p.13) based on vehicle sizes. From this table, the driving distance can be distributed with corresponding interval of time for a day. Further, the State of Charge values may be determined from the current and historical data.

Vehicle Size	Average daily distance covered by the vehicle			Proportion 2008	Proportion 2020
	(1-20km)	(21-60km)	(>60km)		
Small	9.9 km (37%)	36.7km (39%)	133km (24%)	53%	60%
Medium	9.9km (33%)	37.2km (38%)	144.6km (29%)	24%	30%
Large	11.1km (30%)	40.5km (38%)	143.7km (33%)	24%	10%

Table 3 Driving Profiles of vehicles

A test scenario in any future extension may use these criteria for system analysis.

3 Theory of Voltage and Frequency in Power Distribution Grid

In this chapter, the basics of voltage and frequency stabilization are discussed. One of the control methods, droop control, can be used to control the injected power at PCC for stabilization. This method is briefed in this section. The last part of the section introduces the German GC based on which a simple model is studied in the forthcoming chapters.

3.1 Power relation to Voltage and Frequency

The frequency of a grid is dependent on the active power and the voltage of the grid is dependent of the reactive power. It is important to keep these two parameters, i.e., the voltage and frequency of the grid close to their normal values to maintain satisfactory operation of power system. In a simple case considering the whole power network, an Automatic Voltage Regulator (AVR) suffices to keep the voltage on target. The speed governor of the generator suffices to keep the frequency close to normal value by changing the load demand as needed.

At the PDG – PCC, it is required to control the voltage fluctuation through either injection or absorption of reactive power supported by PV or a load and to control the frequency change through absorption or injection of real power, P supported by either PV or load. The related equations (3.1) to (3.4) are derived from (cf.[42].p.20); (cf.[39].p.161); [55].

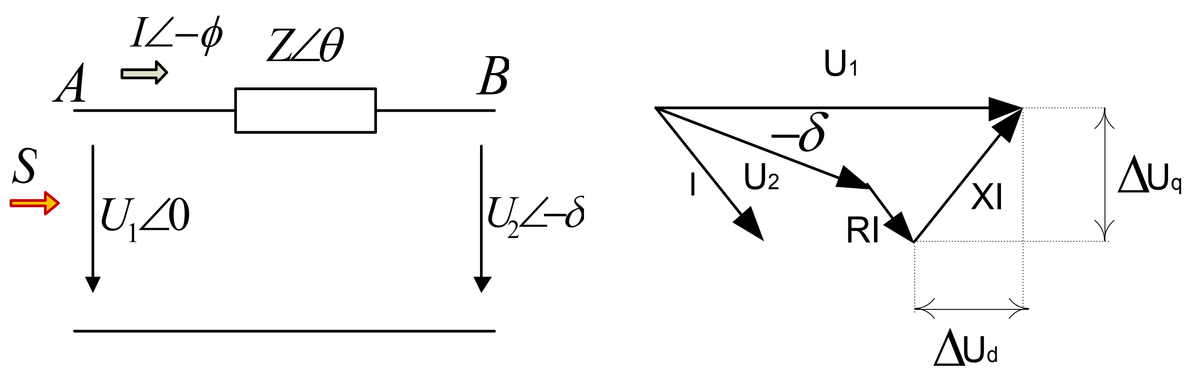

Figure 6 Power flow through a line (single line and phasor representation)

A and B are two different points considered at generation and distribution end of the single transmission line (2 node or 2 bus system). The power transfer along the line is derived in sinusoidal state. U_1 and U_2 are voltages at A and B. S is the complex power that is transferred from the sending end to receiving end. It's a combination of real and reactive powers whose units are in (W) and (VA). δ is voltage angle also termed as torque angle. ϕ is the power factor angle at the point A. R is resistance of the line, X is reactance, Z is impedance. Q is reactive power. The active and reactive power flowing into the line at point A in Figure 6 is,

$$P = \frac{U_1}{R^2 + X^2}\left[R \cdot (U_1 - U_2 \cdot \cos\delta) + X \cdot U_2 \cdot \sin\delta\right] \tag{3.1}$$

$$Q = \frac{U_1}{R^2 + X^2}\left[-R \cdot U_2 \cdot \sin\delta + X \cdot (U_1 - U_2 \cdot \cos\delta)\right] \tag{3.2}$$

When the power flowing through the line in Figure 6 is considered inductive,

$$P = \frac{U_1 U_2}{X_l}\sin(0-(-\delta)) \tag{3.3}$$

$$Q = \frac{U_1 U_2 \cos(0-(-\delta)) - U_2{}^2}{X_l} \tag{3.4}$$

Voltage instability occurs when the power system is unable to maintain steady voltages at all buses. Also, the voltage instability stems from the attempt of load dynamics to restore power consumption beyond the capability of the power system (cf.[40].p.5). A power system subjected to a disturbance may be unable to return to a state of equilibrium once the maximum transferrable power limit has been reached after which the system is pushed toward voltage instability. In this state, the load restoration mechanism leads to a reduction in power consumed rather than the expected increase in power consumption; this is a definite indication of voltage instability [41]. The load is the main driver of this form of instability. Consider the one line diagram of a power system including an interconnected microgrid shown in

Figure 13, where the total load in the microgrid is represented with a single motor at the PCC bus, and other loads are represented with a static load.

There are several articles that discuss efficient droop controller's designs to increase robustness of the grid in presence of the nonlinear loads (such as EVs) within weak grids (cf.[42].p.20). Further, Electric vehicle impact in particular has been the interest for many researchers. This chapter discusses the strategies, scenarios and methods available in literature to control the EV and PV grid impacts on a broader base in the forthcoming chapters.

In the previous section, the relation of voltage and frequency on power at the PCC is discussed. This section elaborates the influence of feed-in active power and injection/ absorption of reactive power to control the voltage at PCC. In the Figure 7, the point S is at the source or transmitting end and the voltage at this point U_S can be assumed as constant. At high voltage levels, the grid voltage is controlled through different electrical equipments and compensation units. So there are very small variations. However, in an LV distribution line, shown as point L (PCC), the voltage magnitude U_L varies. Voltages deviation corresponding to S_L in different cases such as with and without loads, with and without PV is shown. [46].

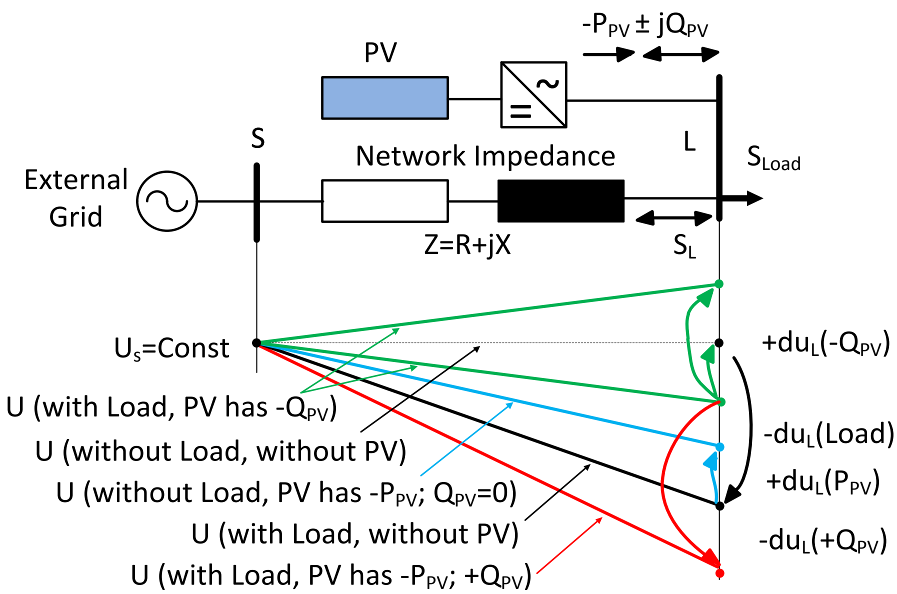

Figure 7 Voltage deviation at PCC in the LV side [46]

The active power feed-in is P_{PV} and the reactive power provided is represented as Q_{PV}. S_{SC} is the short circuit apparent power whose impedance angle is φ_{SC} at the PCC 'L'. S_L is the apparent power at point L. Under normal steady state conditions, the active power flows from the source to the load. Its direction may not be controlled but the amount of power flow can be altered based on the reactive power injected by PV inverters. Due to this reactive power control at PCC, the voltage magnitude can be influenced.

3.1.1 Droop Control

The distributed generators have the potential to deliver reliable power that can be strategically planned. Through droop control, the system frequency and system voltage can be controlled. The frequency deviation signal is used to set the power output of the converter. However, there are several limitations for this use of frequency deviation alone. The drawbacks count slow transient response, unbalanced harmonic current sharing, frequency and amplitude deviations and high dependency on converter output impedance. Refer the droop characteristics of a conventional system for frequency deviation shown in Figure 8 (cf.[55].p.590). The representation relates to the steady state speed versus the load characteristic of the generator unit. The ratio of speed deviation or frequency deviation (Δ f) to change the valve/gate position of power output (Δ P) is expressed in percentage R as,

$$R = \frac{\Delta f}{\Delta P}$$

ω_{NL} *is the steady state speed at no load*

ω_{FL} *is the steady state speed at full load*

ω_0 *is the nominal or rated speed*

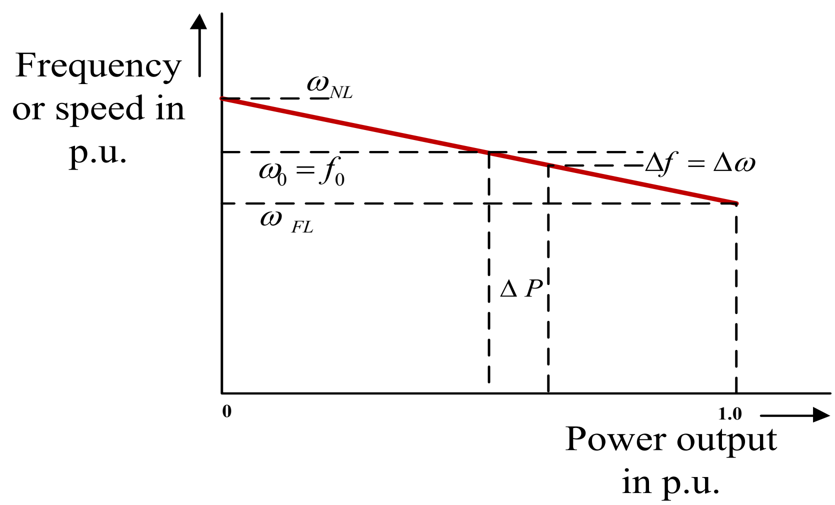

Figure 8 Droop characteristics of power input for a frequency change at PCC

It is possible for a VSC to change its output voltage that could be initiated through a control over the PV's output voltage angle through droop. Since every VSC is connected to an output inductance value, the real and reactive power injection from the PV source is controlled through the change in voltage magnitude and its angle. [49].

3.1.2 Angle Droop Control

The instantaneous power passes through a low pass filter to obtain the average values of real and reactive powers P and Q. The VSC does not directly influence or control the microgrid voltage at the bus $V_t \angle \delta_t$. From the formulation it can be inferred that a change in the angle difference ($\delta - \delta_t$) influences a change in the real and reactive power fed into the grid. So the real power can be controlled by controlling δ and the reactive power can be controlled by controlling the voltage magnitude. To simplify the formulations, the power requirement can be distributed among the PV's based on the conventional droop or change in the voltage magnitude and angle as given below.

$$\delta = \delta_{rated} - m \times (P - P_{rated}) \tag{3.5}$$

$$V = V_{rated} - n \times (Q - Q_{rated}) \tag{3.6}$$

When the PV supplies its loads with a rated power level of P_{rated} and Q_{rated}, then V_{rated} and δ_{rated} are the PV's rated voltage magnitude and angles respectively. The coefficients m and n indicate the voltage angle drop corresponding to the real power and the voltage magnitude drop corresponding to the reactive power respectively.

$$Droop = \Delta f / \Delta P \quad \text{[pu]}$$

The conventional droop control method is given in [49]

$$\omega = \omega_s - mP \tag{3.7}$$

$$V = V^* - nQ \tag{3.8}$$

Here, m and n are the droop coefficients, ω_s is the synchronous frequency ($2\pi f$), V is the converter output voltage magnitude, V^* is the rated voltage, ω is its frequency, P and Q are the active and reactive power supplied by the converter. The frequency and voltage are controlled by the P-Q output of the PV sources.

3.2 **Introduction to the Grid Codes**

PV utility connected systems are increasing in Europe and utility has responded through several interconnection requirements to support grid operation and stability. In prior to 2009, the PV grid tied generators were not permitted to participate during faults and hence were disconnected during grid faults. Since early 2009, the increase in grid tied PV units necessitates a situation where the system needs to remain in connection with the grid during normal condition and during disturbances [34] [44]. This section elaborates the German Grid Codes for PV grid integration at LV line. Two requirements that must be considered are:

- Steady state condition: The PV generators will participate in the steady state voltage control to keep the slow voltage changes within acceptable limits. PV units must be able to provide grid support by injecting reactive power and contribute to voltage control.
- Dynamic network support: This is the voltage control related to a transient condition such as voltage dips. It is aimed to avoid disconnection of grid tied PV units as it feared that immediate disconnection of many such units might collapse the grid. At the time of certain grid faults, the PV generators will stay connected to the grid and inject short circuit current

PV systems are mostly connected to the LV and MV lines of the Power Distribution Grids. Hence, it's a demand to focus on grid stability at LV/MV networks. Table 4 shows the basic requirements for grid tied generators in order to be integrated with the network. This study will include analysis over the following in the presence and absence of a delay in the inverter fed power at PCC.

- Active power control for change in frequency
- Static voltage support with reactive power

- Voltage support in the presence of a fault

Voltage level	Reactive Power Supply	Frequency Band	Active Power Derating /Hz
LV (<10 kV)	$0.90_{lagging}$ to $0.90_{leading}$	47.5 ←→ 50.2 Hz	Reduction gradient 40%

Table 4 New Requirements for grid tied generator [45]

3.2.1 Active Power Control

The PV must be able to reduce its power output in case of over frequency. This ability allows the network operator to temporarily limit the feed-in power or even disconnect the plant.

The plant must be capable of reducing the power output on a reduction gradient of 10% steps of the agreed rated output power. According to Figure 9, the PV will have to reduce the output power if the system frequency is beyond 50.2 Hz. The power reduction must follow a 40% per Hz gradient of the instantaneous available power, ΔP. The output power is allowed to increase only when the frequency reduces below 50.05 Hz. The maximum and minimum limits are 51.5 Hz and 47.5 Hz respectively and whenever the value exceeds the limits, the PV is disconnected from the grid.

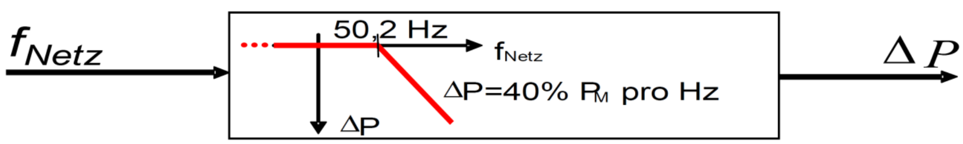

Figure 9 Active power reduction GC for PV under overfrequency condition [34]

3.2.2 Reactive Power Control for Static Grid Support

The MV and LV grid requires a static grid support of reactive power injection to maintain voltage stability ie., to enable normal operation of the grid under slower voltage changes. Whenever the DSO demands operational requirements, the PV will have to supply reactive power for grid support. At the PCC, the PV has to ensure that every operating point maintains a displacement factor between the range, $\cos\phi = 0.95_{under\ excited}$ to $0.95_{over\ excited}$.

Reactive power feed-in from the inverter produces losses in lines and transformers [34]. The investigated reactive power supply methods are [46]. The set point value is set as shown,

- Fixed displacement factor $\cos\phi$
- Variable displacement factor depending on the active power $\cos\phi$(P): The power factor depends on instantaneous active power injection as shown in Figure 10.
- Fixed reactive power
- Variable reactive power depending on the voltage Q(U)

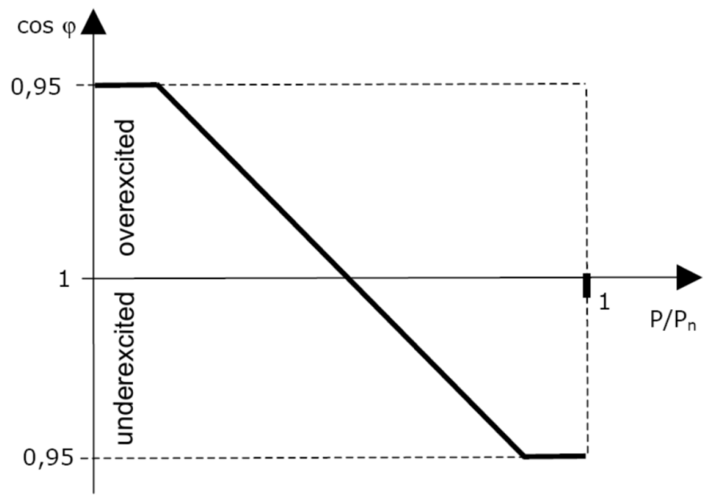

Figure 10 An example to show ϕ(P) characteristic

The nominal voltage-supporting controller, Q = Q(U), is graphically depicted in Figure 11. The controller is a linear approximation of the voltage-supporting controller as specified, e.g., in the German GC for PV installations 46. Here, a change in voltage ΔU is supported by a reactive power injection Q (U). The reactive current deviation is mentioned as ΔIre. The controller may include a deadband value up to ±0.1 p.u along with a droop (or) gain setting of range 0 to 10 p.u. By default, the droop value is set to 2 p.u.

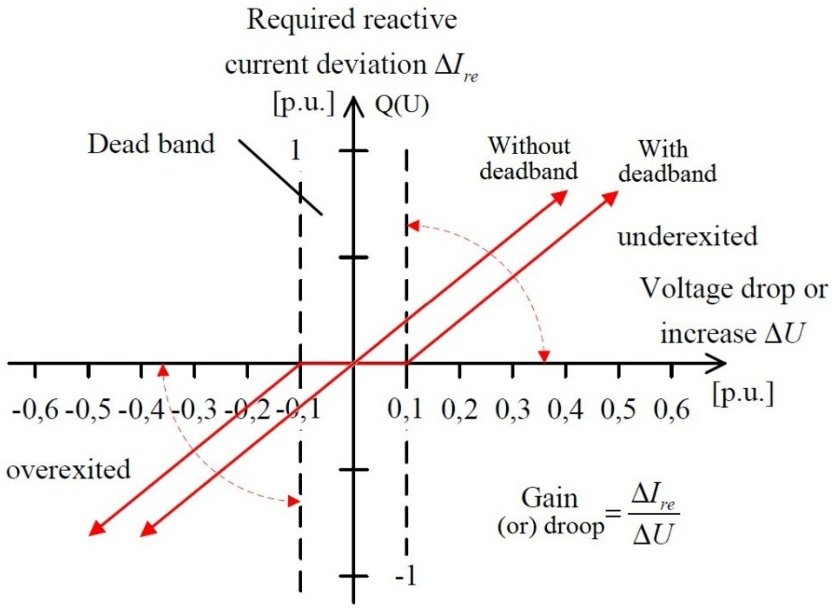

Figure 11Graphical representation of droop controllers with / without deadband

3.2.3 Dynamic Grid Support

Dynamic voltage support refers to the requirements of grid tied PV that needs to be fulfilled under a fault condition or grid disturbance. The requirements are discussed [43][34].

<u>Fault Ride Through</u> (FRT): This requirement describes the voltage stability of a system during a voltage drop that is caused due to a fault condition. The FRT criterion further defines the response of the grid tied PV system at PCC during and after a disturbance. This is important considering the amount increase in PV penetration into the PDG. The dynamic grid support ensures that the generating plants have to be able to

- Stay connected to the during a fault
- Support voltage fluctuation by providing reactive power during the fault
- Consume less or same amount of reactive power once the fault is cleared

This consists of two types of generating plants. The first is a synchronous generator directly connected to grid and second type is the DG plants such as PV. Type 2 alone is considered as this thesis focuses on DER, Figure 12 shows the limiting curves during a fault. Even in the case of a 0% voltage drop due to a fault, the system must not disconnect PV from the grid when the duration of fault is ≤ 150 ms. In Figure 12, there is no requirement for the PV to remain in network below the blue line (borderline 2). If the voltage drop is at values above the borderline 2 and below the borderline 1, PV shall pass through the fault without disconnecting from the network. The simulation in this thesis follows an analysis in presence of a faulted condition. However, due to the time constraint, the simulations have not been associated to the GC requirements. This is a possible future extension. Any further analysis that includes the study of the same system in accordance to FRT would be beneficial in adapting it to the scenarios.

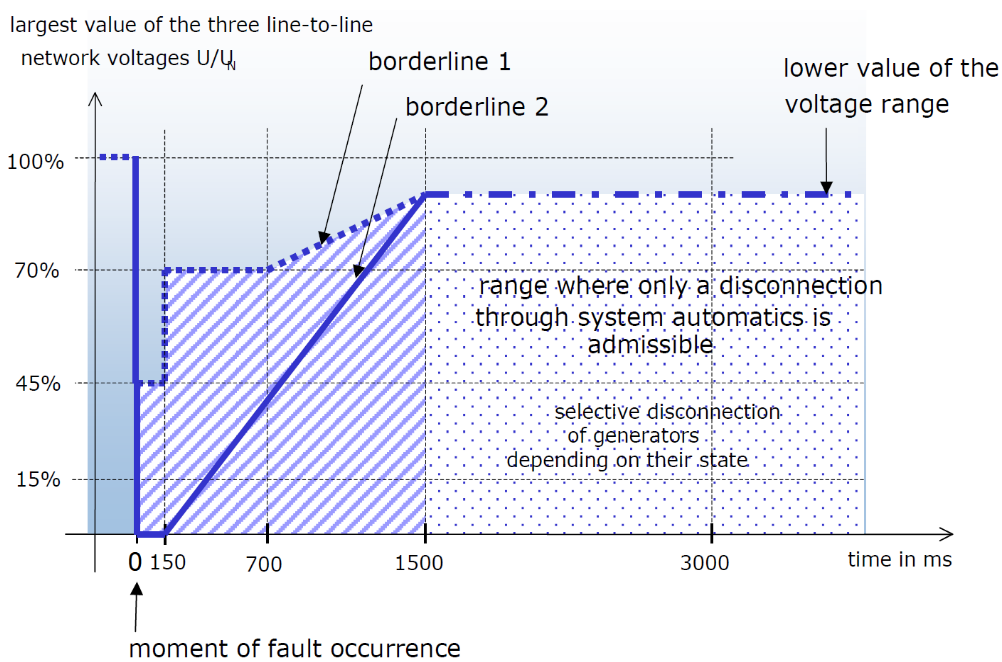

Figure 12 Fault ride through capability of system for German GC [34]

3.2.4 International Grid Codes

The first three parts of section 3.2 elaborates the German GCs. There are several other standards developed by international organisations to promote a uniform-based requirement. Such standards aim to boost up the PV market further to facilitate the interconnection of distributed systems among neighbouring countries. This section briefs some of the important points of such standards (cf.[43].p.31-34),

- IEEE 1547 – Interconnection of Distributed Generation. This standard is in accordance to the IEEE 929-2000 and the UL 1741 covering recommended practices for utility interface of small-scale PV systems. It also lists important safety and grid performance requirements that influence several PV inverter technologies. IEEE 1547 focuses the technical specifications and testing standards, general requirements, response to abnormal conditions, power quality, installation evaluation and other requirements for interconnected generators up to 10 MW.

- IEC 61727 – Characteristics of Utility Interface. This standard is specifically for PV grid tied systems operating in parallel with the utility and the PV systems interconnected to the distribution system. Another standard, IEC 62116, defines the testing procedures as cited in the IEC 61727.
- EN 50160 – Public Distribution Voltage Quality. It defines the main voltage parameters and its permissible deviation ranges at the PCC in the MV and LV network under normal operation. A few parameters are of interest for designing the control of PV inverters according to this standard that is expected to fulfill 95% of testing period. For the remaining 5% of the period, other wider ranges are taken into account.
    - The voltage harmonic levels. Maximum THD is 8%.
    - The voltage unbalances (three-phase inverters). Maximum unbalance is 3%.
    - Voltage amplitude variations. Maximum $\pm$ 10%
    - Frequency variations. Maximum $\pm$ 1%
    - Voltage dips: duration $<$ 1 s at 60 % voltage dip

4 State Space and Component Model of the Test System

In this chapter, a simple two bus model is described in its equivalent circuit for obtaining its corresponding state space model. When the system is obtained in state space representation, it is efficient from a computational standpoint for computer implementation. The formulations and linear representation are briefed for the VSC of PV inverter tied to grid and the short transmission line that are used.

Mathematical modeling is pursued to improve the system design targeting certain system behaviours. The earlier chapters discuss the importance of static voltage and frequency control at the PV end to maintain the system stability. To evaluate these characteristics, a simple PV grid tied setup is modeled and analyzed in a simulative environment. This chapter elaborates the linearization of the model (i.e., state space model) with two grid-tied PV connected to a load at PCC whose basic schematic is give in

Figure 13. This figure shows the power flow direction from PV to the micro grid and from the PCC to the loads. Essential parts of the system are represented in equivalent differential equation and state space matrix forms.

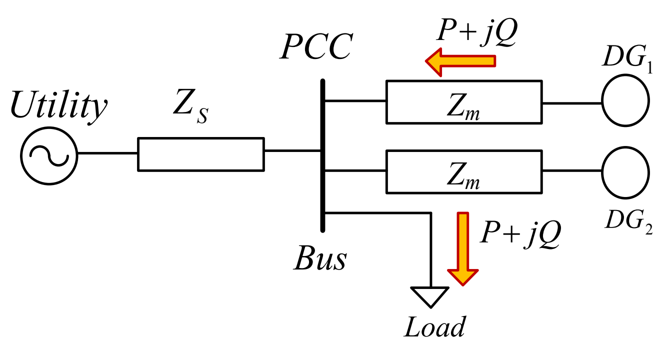

Figure 13 Basic schematic of grid tied PV with load

The line connected from the PCC to the utility is represented as source impedance, Z_S that is elaborated in Figure 14 with inductive reactance and resistance. The output impedance of VSC is denoted by jX_f. The motor or load impedance, Z_m is a line representation consisting of inductive reactance. For transmission lines R/X ratio is low and hence X is predominant. However, this thesis is a distribution line where R is predominant. The direction of power flow is shown that DG_1, DG_2 (PV inverters) supply the power to grid and load through PCC.

The PV grid tied inverter model consists of three main parts, the PV panel that can be considered as a DC voltage source, voltage source converter, a line connection the PCC represented with an impedance 'L' all of which are connected to the external grid.

Figure 13 represents a basic schematic of the grid tied PV system. Figure 21 and Figure 14 show a simple model and its equivalent circuit considered for analysis in this thesis. P, Q represents real and reactive power supplied by the PV. P_L and Q_L are the real and reactive power demand of the load. The line resistances are denoted by R_1, R_2 and the inductances are represented as L_1 and L_2. P_1, P_2 and Q_1, Q2 represent the real and reactive power supplied by the two DG's. Figure 14 has two inverters VSC 1 and VSC 2 that are supplied by a common DC bus capacitor of voltage V_c.

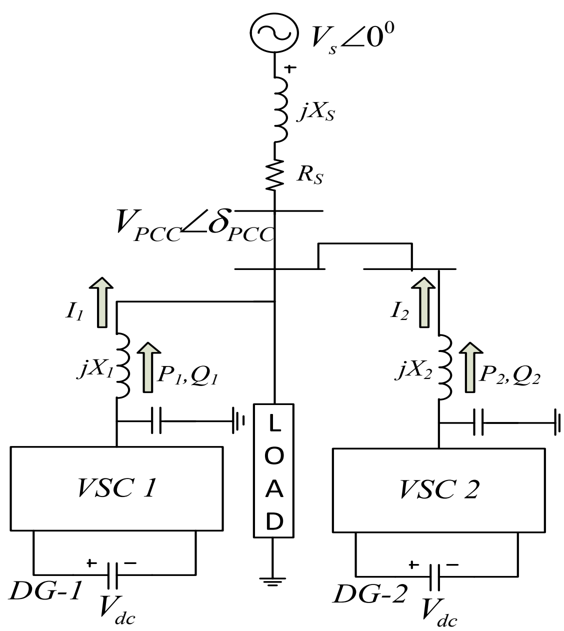

Figure 14 Electrical topology of the test system

4.1 Converter and Filter

The state of art converter strategies are analyzed and a common model whose circuit topology is shown in Figure 15. The schematic consists of the PV panel represented as a DC source connected to a storage element either capacitor or inductor and then connected to an inverter circuit. This is connected to the utility or external grid through DC bus bar and capacitor element. An equivalent circuit is drawn including the main circuit components after which its differential equations are calculated for state space analysis.

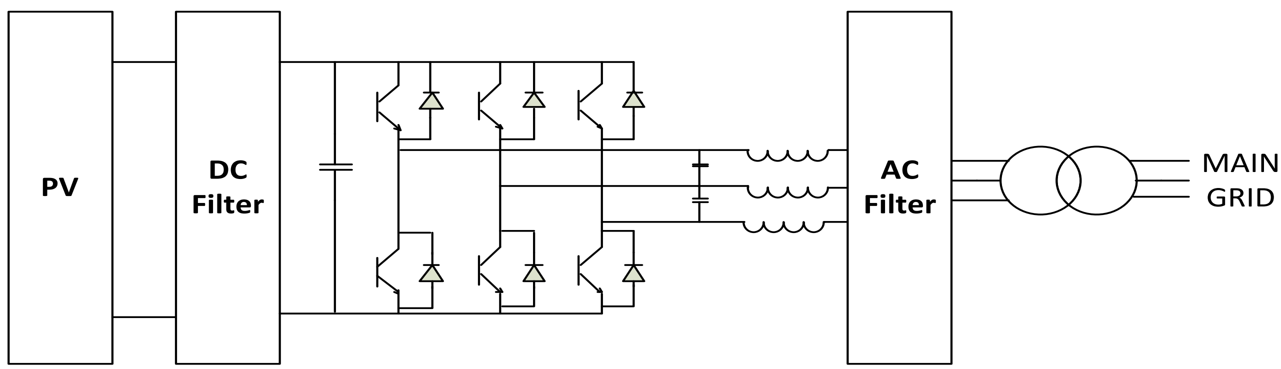

Figure 15 Equivalent circuit of a grid tied PV system with DC filter and Inverter

The PV is assumed to be an ideal DC voltage source V_{dc} that is connected to the VSC. A single phase equivalent circuit for the VSC is given Figure 16 [49]. Commonly used voltage source converters for PV and grid connection are [49-51] (cf.[43].section 2).

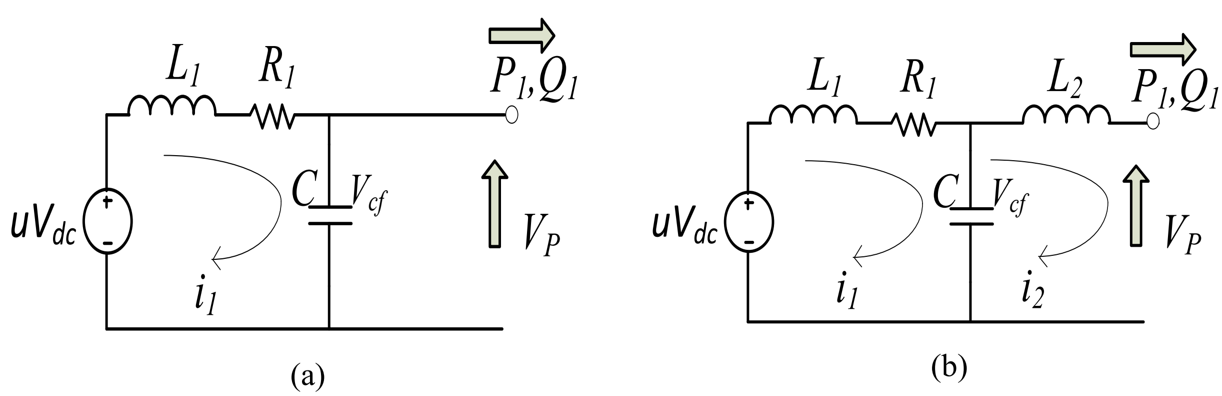

Figure 16 phase equivalent circuit of VSC ((a) LC and (b) LCL filter types)

u, seen in the Figure 16 along with the source V_{dc} is a control variable controlled by PWM signals of IGBT,

$$u \in \{-1,0,1\}.$$

First order differential equations of the equivalent circuit with LC filter shown in Figure 16 is derived to be

$$L_1 \frac{di_1}{dt} = uV_{dc} - R_1 i_1 - \frac{1}{C}\int i_1 dt$$

Since, $i = \frac{dq}{dt}$, the following equation are derived to be

$$uV_{dc} = R_1 \frac{dq}{dt} + L_1 \frac{d^2q}{dt^2} + \frac{q}{C}$$

$$L_1 \frac{di_1}{dt} = uV_{dc} - R_1 i_1 - \frac{1}{C}\int i_1 dt.$$

For VSC with LC filter the following state space equations are represented in matrix form:

$$\begin{bmatrix} \dot{x}_1 \\ \dot{x}_2 \end{bmatrix} = \begin{bmatrix} 0 & \frac{1}{C} \\ -\frac{1}{CL_1} & -\frac{R_1}{L_1} \end{bmatrix} \begin{bmatrix} x_1 \\ x_2 \end{bmatrix} + \begin{bmatrix} 0 \\ \frac{V_{dc}}{L_1} \end{bmatrix} u. \tag{4.1}$$

The filter state vector based on the circuit given is shown in the following equations

There are several voltage control strategies that can be employed on the LC and LCL filter structures shown in Figure 16. The state space description of the system with LC filter is shown in the following equations [52]. Equation (4.2) defines the state vector and (4.3) defines the state space equation.

$$x^T = [v_{cf} \quad i_1] \tag{4.2}$$

$$\dot{x} = Ax + Bu_c \tag{4.3}$$

Where the matrices A and B are

$$A = \begin{bmatrix} 0 & \frac{1}{c} \\ -\frac{1}{L_1} & -\frac{R_1}{L_1} \end{bmatrix} \text{ and} \tag{4.4}$$

$$B = \begin{bmatrix} 0 \\ \frac{V_{dc}}{L_1} \end{bmatrix} \tag{4.5}$$

The state vector and space equation for system with LCL filter is shown in (4.6) and (4.7).

$$x^T = [v_{cf} \quad i_1 \quad i_2] \tag{4.6}$$

$$\dot{x} = A \cdot x + B \cdot u_c + K \cdot v_P \tag{4.7}$$

The matrices A and B can be expressed as (4.7)

$$\text{A}=\begin{bmatrix} 0 & \frac{1}{c} & -\frac{1}{c} \\ -\frac{1}{L_1} & -\frac{R_1}{L_1} & 0 \\ \frac{1}{L_2} & 0 & -\frac{R_2}{L_2} \end{bmatrix} \qquad B = \begin{bmatrix} 0 \\ \frac{V_{dc}}{L_1} \\ 0 \end{bmatrix} \qquad K = \begin{bmatrix} 0 \\ 0 \\ -\frac{1}{L_2} \end{bmatrix} \tag{4.8}$$

Where u_c is the continuous time version of switching function u. Based on the simple model in this thesis, a suitable feedback control law $u_c(k)$ can be computed. In both the above mentioned cases (LCL and LC), u_c is a feedback control which is based on converter switching signal $u = \pm 1$ which is generated through the A and B matrices. One of the several control strategies maybe employed on the available state matrices.

A literature is reviewed that computes the feedback control using output feedback voltage controller and state feedback controller [52]. $V_t \angle \delta_t$

$$X^T = [i_2 \quad i_{cf} \quad v_{cf}] \tag{4.9}$$

Here, the converter output is the same as the voltage across the filter capacitor v_{cf} and the controller action tracks with perfection when the error is within limit [52]. The system parameters are given in the appendix.

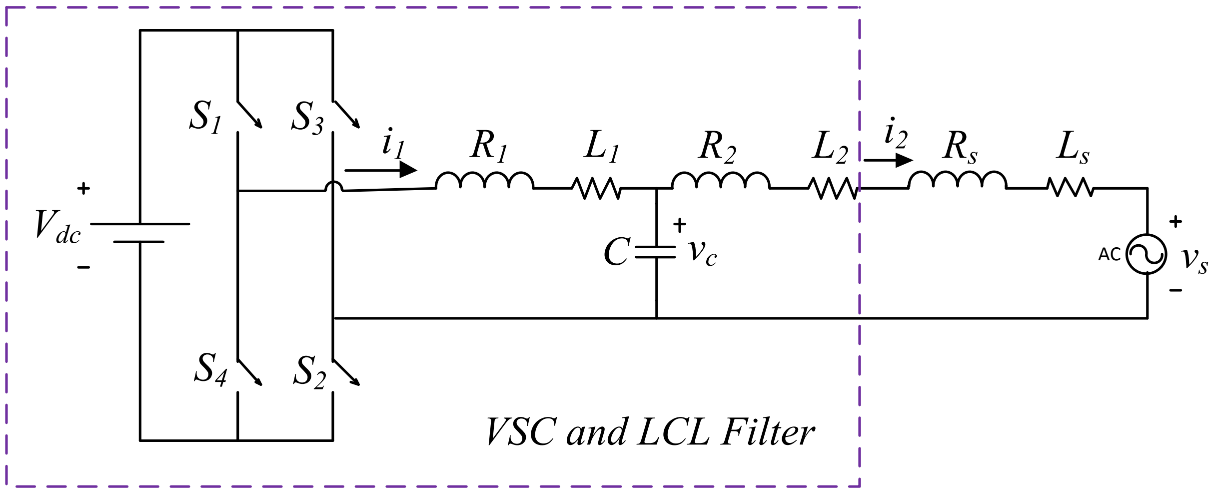

Figure 17 Equivalent circuit of VSC and LCL filter

The equivalent circuit shown in Figure 17 is a combined form of both VSC and LCL filter represented together. R_S and L_S are the series resistance and reactance values in the circuit. The state space input A matrix of the VSC and LCL filter is given as,

$$A = \begin{bmatrix} 0 & \frac{1}{c} & -\frac{1}{c} \\ -\frac{1}{L_1} & -\frac{R_1}{L_1} & 0 \\ \frac{1}{(L_2 + L_S)} & 0 & -\frac{(R_1 + R_2)}{(L_2 + L_S)} \end{bmatrix} \tag{4.10}$$

4.2 Short transmission line model

A short-length line is termed as any line that is lesser than 80 km in length. The shut capacitance effect is negligible here. The resistance and inductive reactance are alone considered. Assuming balanced conditions, the line can be represented by the equivalent circuit of a single phase with resistance R, and inductive reactance X_L in series (series impedance), which is shown in Figure 18 and Figure 19 (cf.[53].p.47).

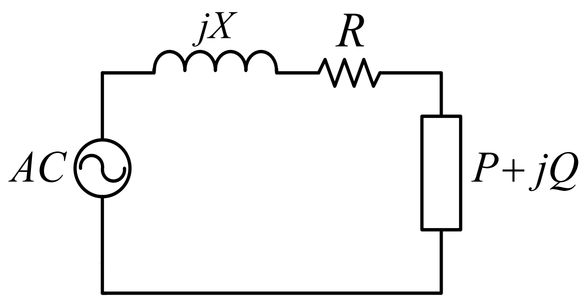

Figure 18 Equivalent circuit of short transmission system

The line losses are represented by their series L and R (inductance and resistance) and the shunt C and G (capacitance and conductance) values for infinitesimal lengths dz.

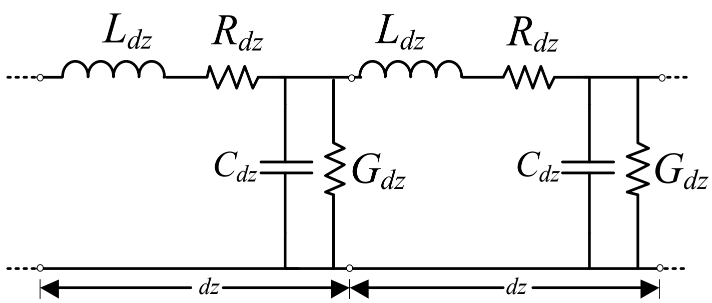

Figure 19 Short transmission line considering line losses

Through a first order differential representation of the above circuit, the system behaviour of voltage and current can be analyzed. ω is the frequency $2\pi f$.

$$\begin{cases} \dfrac{dV}{dz} = -j\omega LI \\ \dfrac{dI}{dz} = -j\omega CV \end{cases}$$

4.3 **Solar cell and equivalent circuit**

The building block of the PV array is the solar cell, which is a p-n semiconductor junction that converts solar radiation into dc current using the photovoltaic effect. Figure 20 shows the equivalent circuit of the solar cell consisting of a current source, a diode and resistances in series and parallel [54]. PV cell is a non-linear device and can be represented as a current source in parallel with diode as shown in the circuit Figure 20. The practical PV cell model includes the connection of series and parallel internal resistance R_s and R_p.

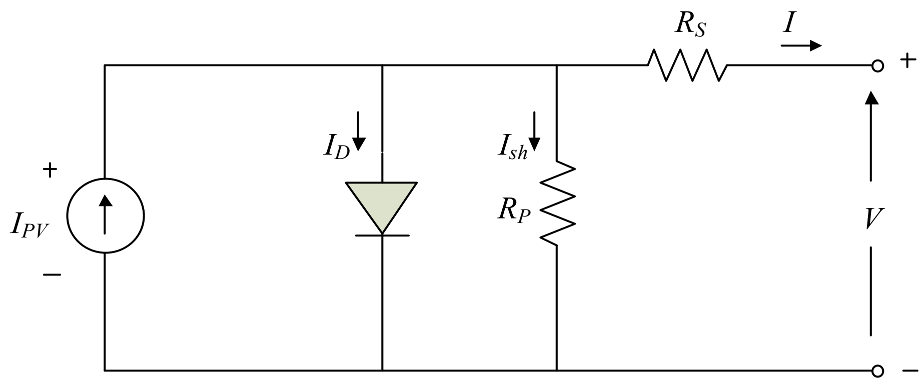

Figure 20 PV equivalent circuit model

The output current in this model is,

$$I = I_{PV,cell} - I_{sat}\left(e^{\left(\frac{V+R_sI}{V_t}\right)} - 1\right) \tag{4.11}$$

$$V_t = \frac{AkT}{q} \tag{4.12}$$

$I_{PV,cell}$ = PV cell output current or photovoltaic current

V = *Voltage across the cell*

V_t = *Thermal voltage as a function of temperature T*

R_S = *Equivalent series resistor*

I_{sat} = *Saturation current of the diode of the array*

$N_s kT_c/q$ = *Thermal voltage of array with Ns cells connected in series*

q = Electron charge (1.60217646 e−19 C); k = Boltzmann constant (1.3806503 e−23 J K−1)

T = Temperature of the p-n junction measured in Kelvin K and A = Diode ideality constant

The equation 4.11 is derived from the short circuit, maximum power point and open circuit values of VI curve of the single diode model shown in Figure 20.

Active power calculation for the test system

PV cells are generally grouped together to form larger units called models or arrays, in a combination of serial and parallel networks to provide the desired output current and voltage. Let the arrangement of number of solar cells be in $N_{p\text{-}parallel}$ and $N_{s\text{-}series}$, The network analyzed in this thesis contains a PV module set to STC with V_{mpp} as 35V and I_{mpp} as 4.58A. The active power of 448.84 kW generated by the panel is calculated based on the 20 modules per string which is counted for 140 modules in parallel as shown below.

$$35V \times 20 Modules_{series} = 700 \qquad Active\_Power = V \times I$$
$$4.58A \times 140 Modules_{parallel} = 641.2 \qquad Active\_Power = 700 \times 641.2 = 448.84kW$$

4.4 Further analysis of the simple network

In order to study the stability of a microgrid, one of the suitable methods is to analyze its components through state space models using differential equations. A common reference frame may be chosen for this purpose and the voltages and currents may be converted to DQ reference frames. A simple model with two grid-tied PVs is shown with their corresponding linear quantities in this section. This also includes the controllers for state feedback, droop and a block that connects converter to the grid. Real power and reactive power output of the converter (Δ P, Δ Q) is the input for the droop control. The droop controller sets the voltage reference values and feeds back to the converter. In this system, we are essentially dealing with small perturbations which determine the specific system behaviour for which a linear model is adequate at the PV generator internal buses.

5 System Modeling and Simulative Analysis

The previous chapters have provided a literature and an investigation of a system with the EV and PV elements. This chapter analyzes the theory over a simple model in a simulative environment. For analysis, the simple model is simulated in accordance to the grid codes. It contains one and two inverter cases. A brief description of the software used for simulation along with a detailed description of the model is presented with results.

5.1 Power system simulation tool

Computer models of power systems are widely used for steady state analysis, load flow, dynamic and transient behaviour analysis of power systems. In this thesis, we use DIgSILENT Power Factory software [56] to perform power-system studies.

5.1.1 Model Description

In Power Factory, static generators are available as a generic model. The PV panel and the PV inverter that are available within the static generator are analyzed. The PV inverter has a control setup whose parameters can be altered. It is three phase, connected to an LV terminal of nominal voltage of 0.4 kV and has a system capacity of 0.5 MW.

5.1.2 Base Model

The base PV system built by DIgSILENT is available in the PowerFactory tool, which was analyzed in this thesis work as seen in Figure 21. The PV generator includes a number of control and design features integrated together at an LV terminal with nominal voltage 0.4 kV. The capacity of the system is 448 kW. For the purpose of analysis, simulations are carried out with one and two grid tied inverters in the same network, whose features are discussed. For basic analysis, the model is tuned to abide the German GC ([34], EEG, BDEW). The corresponding DSL codes highlighting important features are documented.

To show the voltage and frequency changes, the system is connected to an external grid and a voltage source in two different cases. Both the external grid and voltage source are inbuilt components.

5.1.3 Photovoltaic Generator

The PV generator is set to inject an active power flow of 448.84 kW during normal steady-state operation. The PV generator's details in Table 7 (in Appendix) are the parameters that can be altered. It is also to be noted that the Power factor is set to 1 at the PCC with LV terminal. The amount of real power flowing at the PCC depends on the MPP and a few other parameters of the PV array which are mentioned in Table 7.

The active power values refer to the AC side i.e., the inverter side, which can inject a maximum of 475 kW. One of the characteristics while designing a PV inverter is to have a maximum limit of active power above the rated value accounting for the operation of inverter at 0.95 PF. The capability curve determines the reactive power limits of the inverter which is shown in the appendix (Figure 40). The parameters of minimum and maximum reactive power injected by the PV grid tie system are given in appendix.

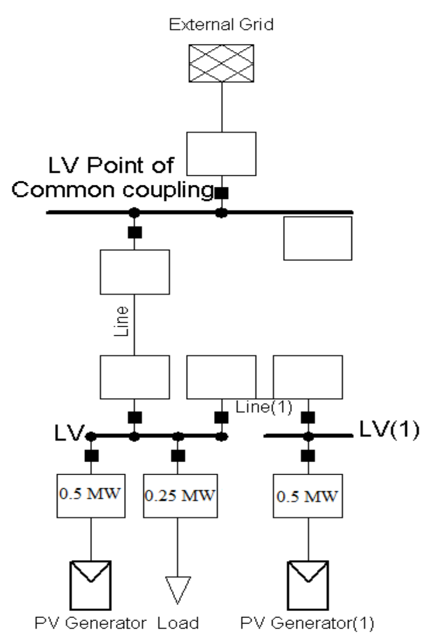

Figure 21 Single line diagram of the test system (DIgSILENT Power factory tool)

5.2 PhotoVoltaic grid tied system

All the features included in the model of the PV inverter are shown in Figure 22. This section provides a brief explanation of the basic parts of the frame that is integrated within the PV generator setup. The BlkDef functions of the PV frame are described in appendix.

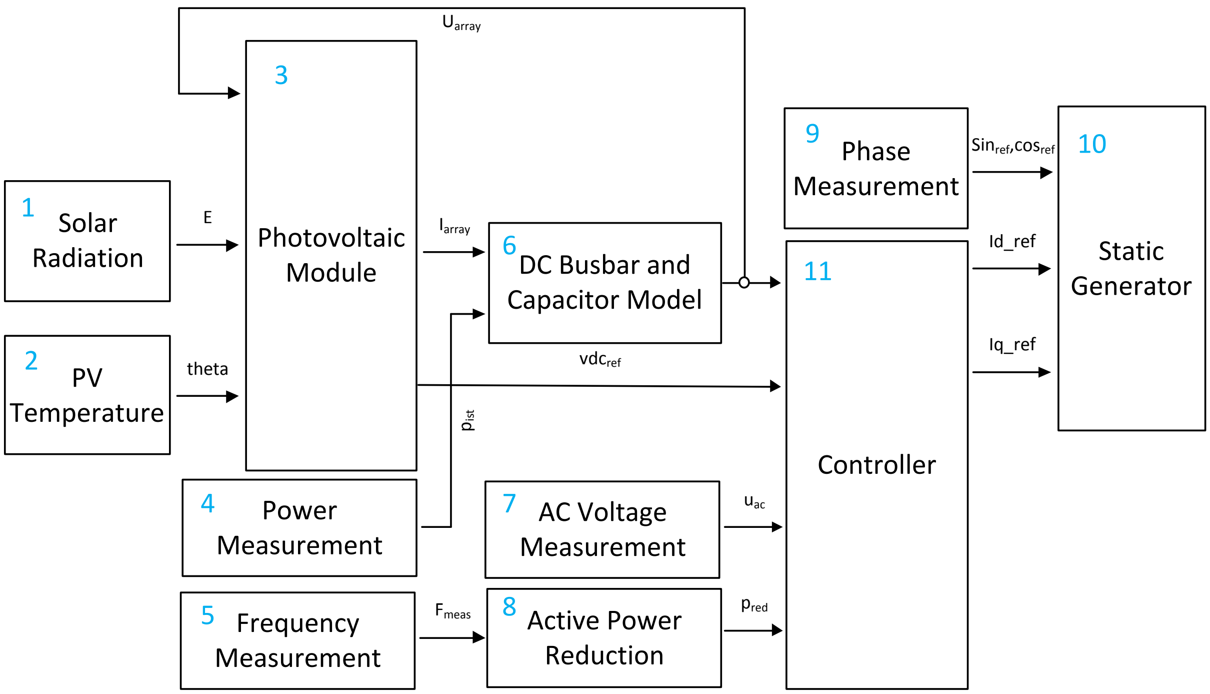

Figure 22 Control frame of PV system

The slots numbered (1, 2, 3, 6) of the control frame are *Solar radiation*, *PV temperature*, *PV model* and *DC busbar & Capacitor model*. These together form the DC side of the inverter. It's only the external factors that might affect these models, such as solar irradiation and temperature reflected by their signals E and theta. An MPP tracking algorithm is used for calculating the output values of array model. *The DC busbar and Capacitor model* represents the connection through a shunt capacitor which inputs the DC side of the inverter.

The *Power Measurement*, *Voltage measurement*, *Frequency measurement* slots along with the *Active power reduction* and *Controller* slots together, count as the AC side of the inverter. The basic control requirements for grid connection are set in accordance to the German GC, as mentioned earlier. The *active power reduction* slot and the *frequency measurement* device (PLL) are responsible for curtailing frequency deviations. The controller slot 11 includes a reactive power support for voltage dips. This is set according to the Transmission code 2007. Currents in dq0 system are denoted as output of the controller id_ref and iq_ref. These are the reference values of active and reactive power injection. The *Phase Measurement device,* slot 9 is a Phase Locked Loop that synchronizes the output signal to that of the grid frequency. The output of slot 9 is connected to the *Static Generator*. The following sections of this chapter elaborate each of these individual slots.

Slot 1: Solar Radiation

The PV power production is fluctuating in nature. Its intermittency increases due to several reasons such as cloud and dust. This intermittency causes voltage variation at the PCC especially in a weak grid [45]. The solar irradiation on the PV array directly influences the array current as a consequence of which, the power output changes. This slot is essential to assess the change of irradiance (dE) per second and integrate them over a period of time. For this thesis, the solar radiation slot is not altered, as this thesis does not count the irradiances caused by cloud effects or wind or dust. Changes in ramp rates can be shown through this slot and analyzed using power measurement device.

Slot 2: Temperature slot

While considering a PV grid connected system, after irradiance the temperature is considered as one of the influential factors of the PV system. This directly alters the voltage of the array. An integrator is used in this slot to represent the potential changes in temperature in the cell or module measured in the range of seconds. No parameter changes have been studied on this slot in this thesis. Simulations are carried out with a constant value of temperature input.

Slot 3: Photovoltaic model

This slot has five blocks of which the main is enclosed in a blue frame. This PV module block describes the basic properties of one PV module out of the entire array. The final values of this particular block are the current and the array voltage at MPP. Inputs in this slot are the operating temperature “theta” and the irradiance “E” that are defined in slots 1 and 2. In addition, the voltage at the DC bus bar denoted as U_{array} is also fed in at the input. The voltage is passed through a low pass filter to attenuate the high frequency signals during abnormal conditions. This is deactivated under normal conditions. Voltage per module is calculated by dividing the filtered voltage by number of serially connected modules.

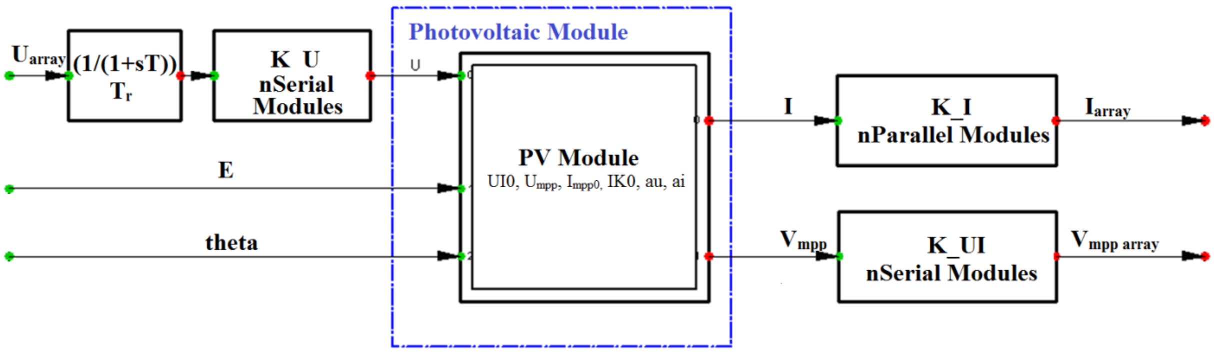

Figure 23 PV module with its input and output blocks

The PV module consists of a built-in MPP algorithm whose basic codes are presented in Appendix. This algorithm calculates the voltage and current at MPP considering temperature and solar irradiation into account. Manufacturer details include a_u and a_i (mentioned in the Appendix) that are used to correct the nominal electrical values which deviate the STC.

Slot 4: Power Measurement

This slot is used to measure power at any desired location. In precise, the PQ measurement device used at any connection point of the PV generator is implemented through this slot. In this model, the active power measured is used as an input value ‘P_{ist}’ to the “DC Busbar and Capacitor model” slot.

Slot 5: Frequency measurement

This is another similar measurement device used for frequency at any desired location. The device used in it is a PLL that is described in the following sections. The output of this slot f_{meas} is input to the “Active Power Reduction” block. This has a constant value of frequency regardless of instantaneous disturbances over a given time period.

Slot 6: DC Busbar and Capacitor Model

This slot represents the connection where the DC side of the inverter is connected to the PV array. This slot consists of two inputs and one output between which four blocks are interconnected. An input I_{array} in this slot is the output of PV model. The second input signal is P_{ist} which is measured in slot 4. The output signal U_{dc} is fed as an input signal to the PV module which is discussed as slot 3.

The function of this slot is to divide the active power measured at a connection point (refer slot number 4) with the U_{dc} to calculate the current in amperes (Amp) that runs through the DC bus. The units here have been transformed from MW to amperes. The resulting DC value is subtracted from the PV array current to find the differential value of the current running in the capacitor (capacitor is in parallel to the DC bus bar). The value of current is transformed to p.u. by considering the nominal base current. While such a transformation, since nominal base current is unknown, it's calculated through the known values of DC voltage and the nominal PV power. The p.u. current is integrated to calculate the voltage across capacitor which is the voltage of the DC bus and input of the inverter. At length, the voltage values are transformed from p.u. to nominal value V.

Slot 7: AC Voltage Measurement Block

The voltage measurement block outputs a signal U_{ac} to the controller, which refers to the measured voltage at the LV bus. This similar block can be used at any required location point for measuring the corresponding voltage at that particular point.

Slot 8: Active power reduction Block

This slot consists of two blocks, a filter and "over-frequency power reduction" block. This slot represents one of the important features to reduce active power injected at PCC. The over-frequency power reduction block is where the German GC is implemented. The inputs are frequency measurement f_{meas} from slot 5 and p_{red} which is an input to the controller. The frequency signal passes through a filter that triggers a function to reduce any excess of active power that is fed at PCC due to over frequency conditions. This follows a 40% gradient drop in instantaneous power value at that time per Hz increase as recommended by the GC.

Slot 9: Phase Measurement Block

This follows a similar explanation provided in Slot 5. This consists of a PLL which is a closed loop structure that contains three major parts. A phase detector, loop filter and a voltage controlled oscillator. An internal oscillator synchronizes by locking phase with a particular grid power signal. This element is capable of measuring frequency and phase of the system voltage. This block is used at the measurement point. The phase detector generates a proportional signal corresponding to the difference between V and V'. The loop filter is a low pass filter that attenuates high frequency AC components. The VCO generates a signal whose frequency is compared to the given frequency and shifted as a function of input filtered voltage produced by the loop filter.

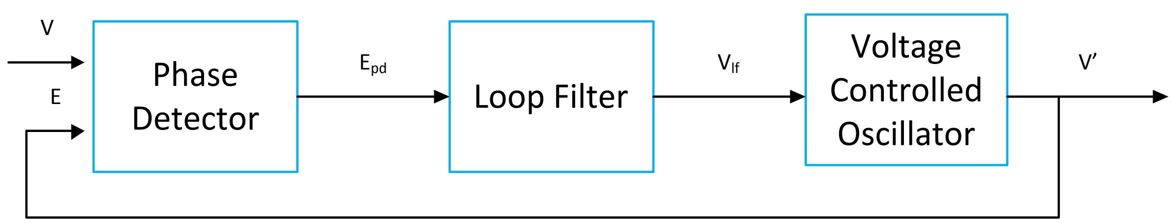

Slot 10: Static Generator

This slot is the static generator component as described in the section 5.1.3, the PV generator is described in the slot.

Slot 11: Controller Block

The controller block has four inputs and two outputs as shown in Figure 24. The output components id_{ref} and iq_{ref} are inputs for static generator slot through which the active and reactive power can respectively be controlled.

<u>For active power control part</u>, the vdc_{ref} value calculated by the PV array model is denoted here as $U_{mpp\text{-}array}$, which is the desired voltage value at MPP at the input end of the inverter (DC side). In order to attenuate high-frequency components, this value passes through a low-pass filter and

then to a lower limit block. The value here is compared with the minimum operating value of the inverter $U_{\_min}$ that is set to a minimum inverter turn off value. Because of this comparison, the voltage value of vdc_{ref0} is always above the $U_{\_min}$. vdc_{ref0} is then subtracted from the actual voltage of the DC side of the inverter, u_{dc}, represented here as vdc_{in} and also with $dvdc_{ref}$. The difference is denoted as dp which is sent through a low-pass filter. Finally, the dpd value enters a PI controller whose proportional gain is K_p and integration time is T_{ip}. The id component that regulates the active power is calculated. The two limiting parameters of the PI controller is, id_min and id_max, and the variable p_{red} from the active power reduction slot. The id parameters represent the minimum and maximum active current limits, while p_{red} is the reduction due to overfrequency.

For the reactive power control, the u_{ac} value is measured by the voltage measurement device which passes through a low pass filter. This value is compared with the voltage at steady state reference value, u_{ac0}. Both these values are compared to result du_{ac}, which represents the deviation in voltage Δu at PCC. The change in voltage is an input signal to the "Reactive Power Support" block, which follows the GC discussed under 3.2. The DSL code shown in the appendix section Figure 44 defines a deadband of 10% of the nominal voltage and also determines the iq component, along with a factor K that is denoted by the droop parameters shown in the appendix section [Table 11].

$$i_q = K|du_{ac}|$$

I_q is written according to the Transmission code 2007. I_{q_max} and I_{q_min} are maximum and minimum reactive power limits for the "Reactive Power Support" block. The I_q and I_d values calculated together with du_{ac} enter the current limiter block, in which the reference values of these components are calculated. Limiter sets the limit for maximum allowed values of absolute current and reactive current for normal operating conditions.

To initiate a delay parameter in the model, the DSL of the active power reduction block and the current limiter of the controller blocks are altered. The altered main codes of DSL alone are mentioned here, and for a detailed DSL code of all the blocks refer the appendix section.

One of the output signals of the controller block is I_{q_ref}. The internal parameter linked to this output signal iq_{out}, is changed by altering its DSL code in the current limiter block. The functions delay and absolute ‘abs’ are added to initiate a 200 ms delay as shown below.

```
iqout=delay(abs(select(i_frt,lim(iqin,-maxAbsCur,maxAbsCur),
lim(iqin,-min(delta,maxIq),min(delta,maxIq)))),0.2)
```

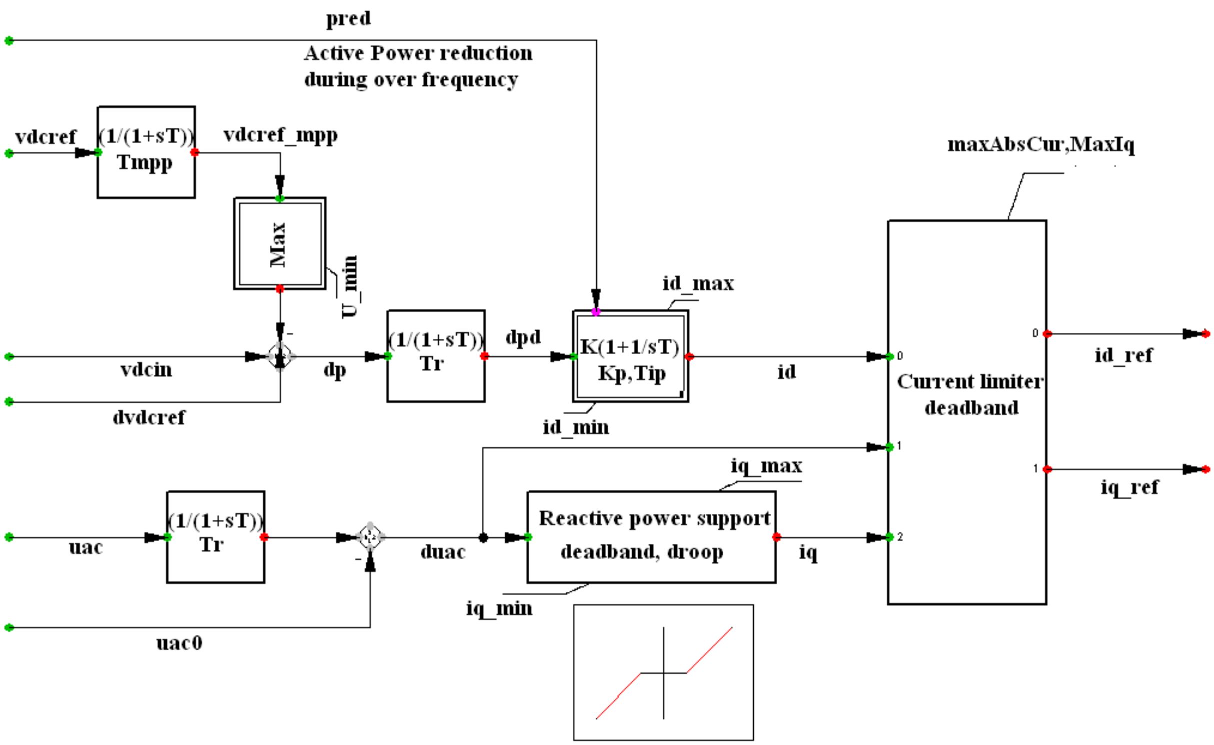

Figure 24 Controller Block of PV grid tied inverter

The simple model used is connected to a weak grid. The rigidity of a grid is determined by the short circuit power ratio, $k_{kl} = S_{SC}/S_{PV\_max}$ where S_{SC} is the short circuit apparent power at PCC and S_{PV_max} is the PV’s maximum apparent power. The terminal’s rigidity based on short circuit power ratio can be used to determine if whether a grid is weak grid or not [46].

Also, by using the equation (2.1),

$$SCR = \frac{V_{Grid}^2}{Z_{weak}S_{rated}} = \frac{0.4^2}{(0.1264 + \mathrm{j}0.06597\ \mathrm{ohm})(0.448)}$$

The SCR value is 2.221 (ie., < 10), the grid of the simple model is considered to be weak [5].

5.3 **Simulation and Stability analysis**

Initially, the active power reduction in the presence and absence of the delay parameters is shown in this section of the paper. Active power curtailment refers to the ability of the generating plant to reduce its power output, as required by the network operator to address the stability issues. The German grid code mentions that the PV generator should reduce its power output when an over frequency occurs [34]. The GC defines over frequency as those values that are above 50.2 Hz. Under such a condition, a reduction in the power injected with a slope of 40% value at that instantaneous time is recommended for every Hz increase.

5.3.1.1 Power flow studies

In power engineering, appropriate Power-Flow study is a tool that involves numerical analysis applied to a power system. This study uses a simplified form of the network ie., one line diagram and per unit system.

The objective of power flow study is to analyze the steady state performance of the system under different operating conditions. In particular, the voltage magnitude, phase angle at each bus and the power flow through each line, including the power consumed at the buses, is the basic power flow question for a given power system. This analysis remains the basis for planning, design and operation of any electrical power systems. Such studies are hence needed to assess the allowed EV and PV penetration level for a given network in order to ensure that the maximum voltage at the point of common coupling (PCC) and lines current carrying capacity are not exceeded.

5.3.1 Time Domain Analysis for active power reduction

5.3.1.1 Active power reduction with and without delay

Frequency of the external grid is changed from 50 to 52 Hz at 0.25 sec that initiates active power injection at PCC. The active power reduction control is set according to the grid code with a gradient of 40% per Hz above specified limit. Active power measured in Per Unit at the PCC is simulated and presented in the Figure 25 to Figure 30. As discussed in the earlier sections, it is expected that a delay in the active power fed at PCC might result in low frequency oscillation. The impact due to the switching time difference between two inverters is also simulated.

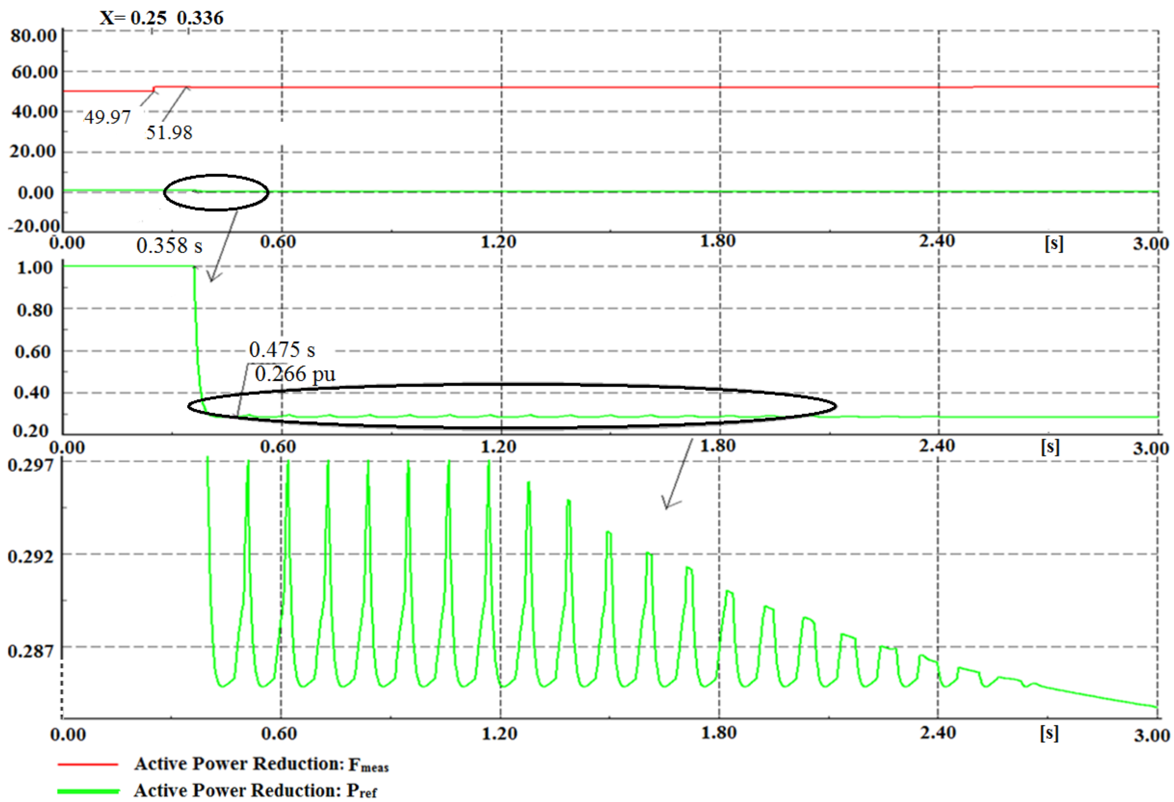

Figure 25 Frequency change and active power reduction with a delay

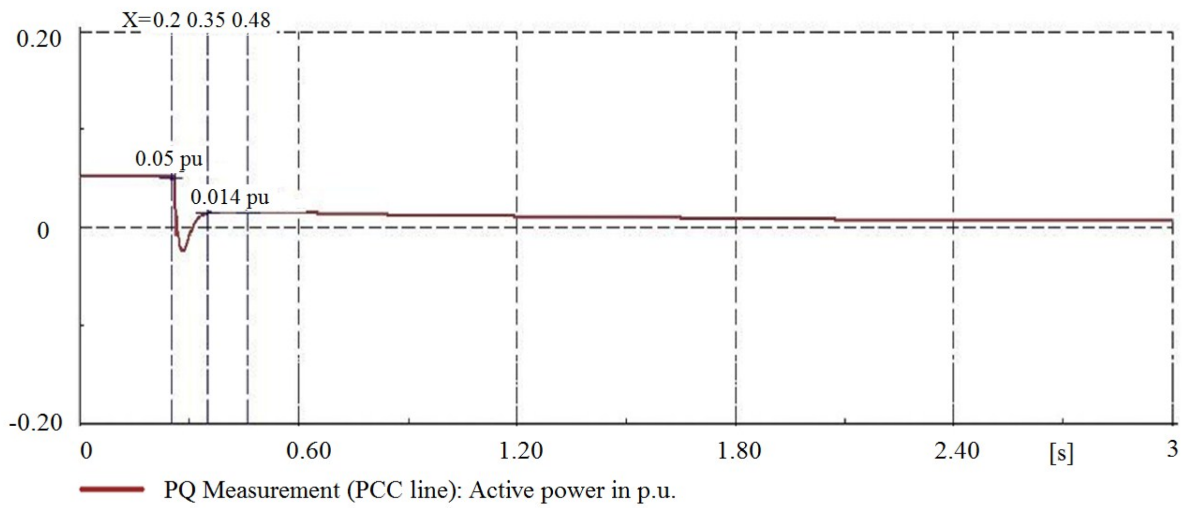

Figure 26 active power measurement (Inverter 1: 0ms; Inverter 2: 0ms) droop 2 (Watt/V)

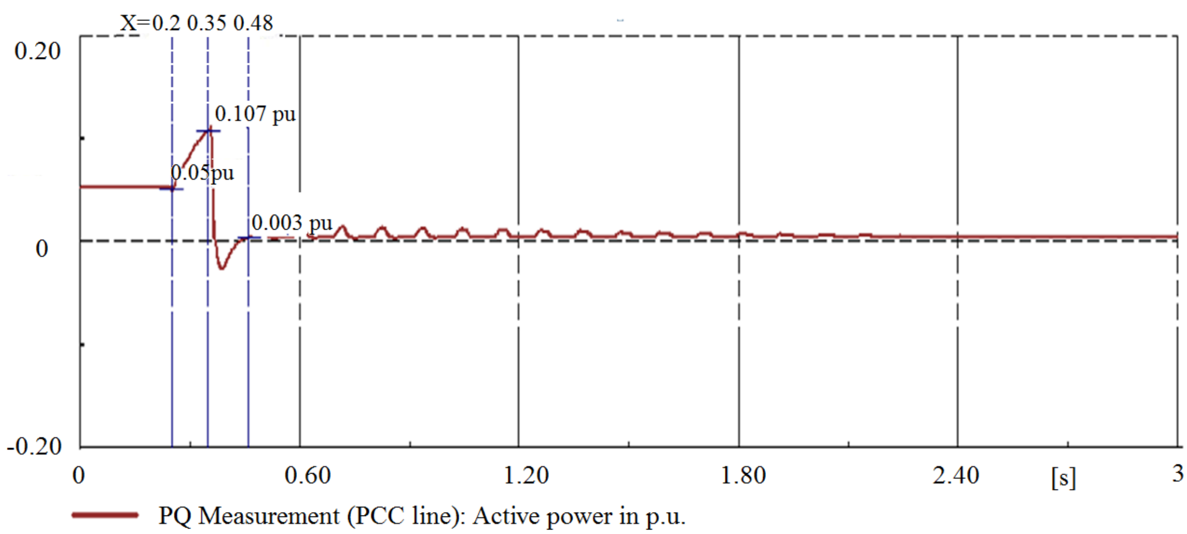

Figure 27 active power measurement (Inverter1 and 2: 100ms) droop 2(Watt/V)

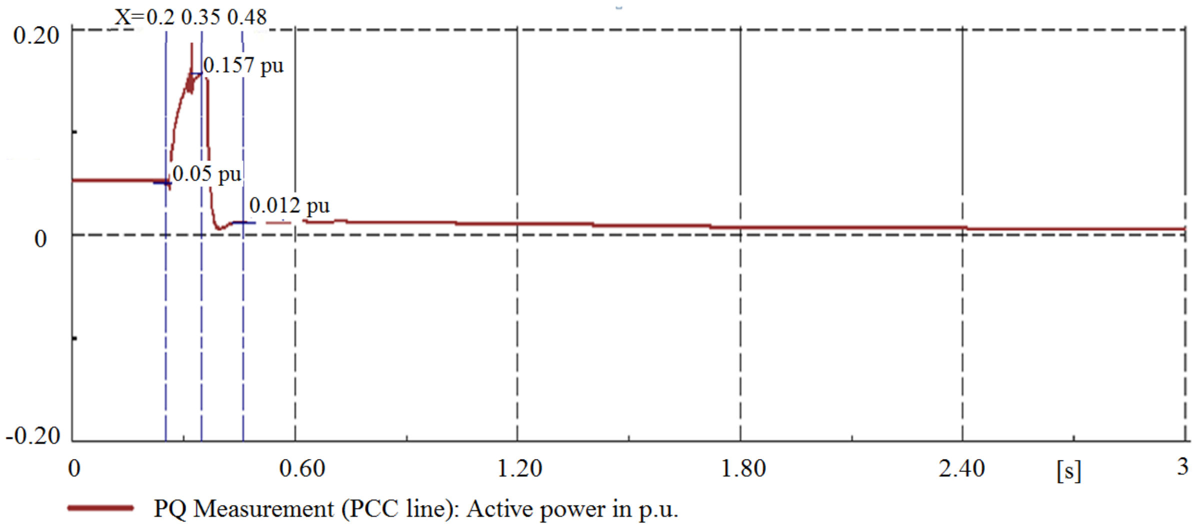

Figure 28 active power measurement (Inverter 1:100ms; Inverter 2:0ms) droop 2(Watt/V)

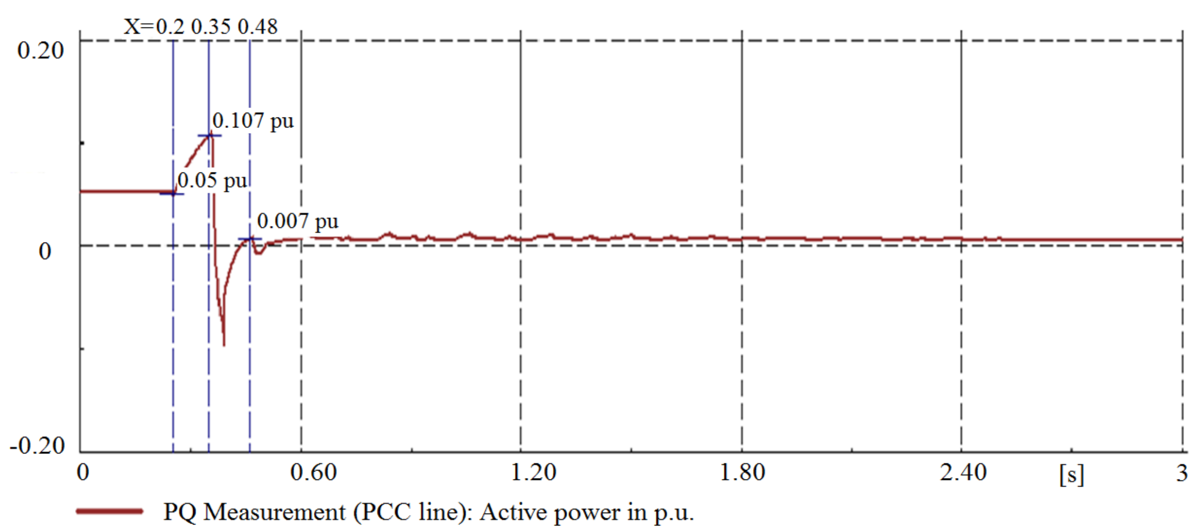

Figure 29 active power measurement(Inverter1:100ms; Inverter2:200ms) droop 2 (Watt/V)

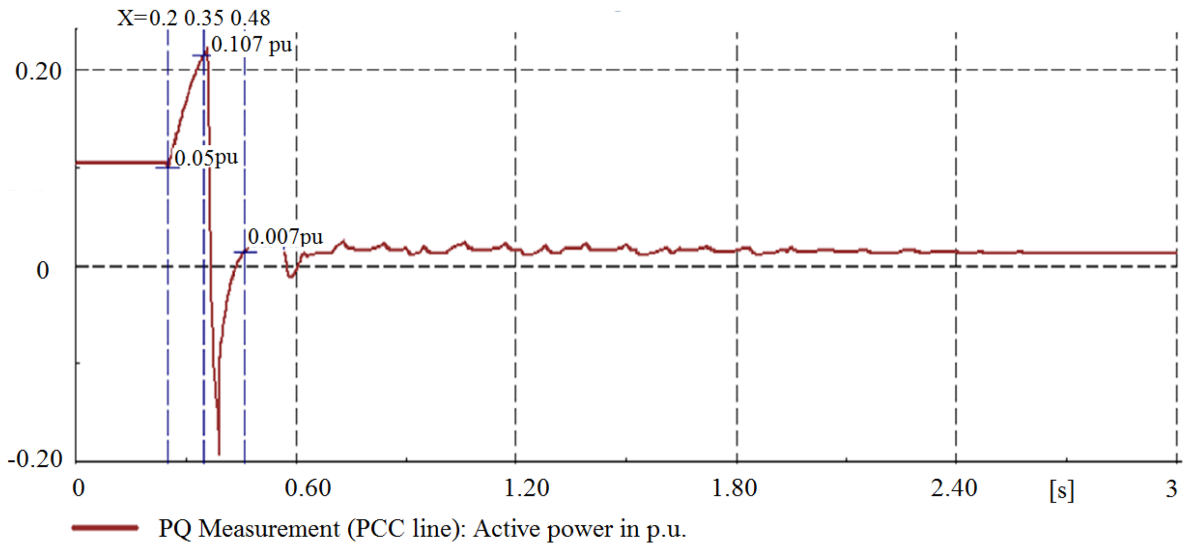

Figure 30 Active power measurement (Inverter1:100ms; Inverter2:300ms) droop 2(Watt/V)

From the above simulations, it is clear that the average system frequency change, when supported with an active power injection causes a pulsating power in case of a transportation delay. The fluctuation at PCC increases with delay, droop values and is dependent on the switching time between two inverters. In the absence of a delay, it can be inferred that there exists a dip in the active power (which is only due to frequency change) without any fluctuations at PCC. A few measures suggested in the section 2.4 with changes in their performance criteria mentioned in the section 2.3 are possible solutions to mitigate this under damped oscillation nature.

5.3.2 Static voltage support with and without delay

Voltage across a grid will change due to the switching of large loads. A set of loads are turned off at 2 sec to initiate a voltage change at PCC. The reactive power fed at this point is controlled by the inverter based on voltage deviation. According the GC, a deadband of 10% and a droop of 2 ($^{\text{Watt}}/_{\text{V}}$) is recommended.

$$Droop = \frac{\text{Change in reactive power injected into the grid } (\Delta Q)}{\text{Change in the voltage measured at the grid } (\Delta U)}$$

The simulations carry a constant droop of 20 ($^{\text{Watt}}/_{\text{V}}$) and a deadband of 0% with different inverter delay periods. The oscillation in reactive power is seen to gradually reduce within a few seconds. However, it depends on the amplitude of oscillation which invariably depends on the voltage droop, deadband and the inverter delay period.

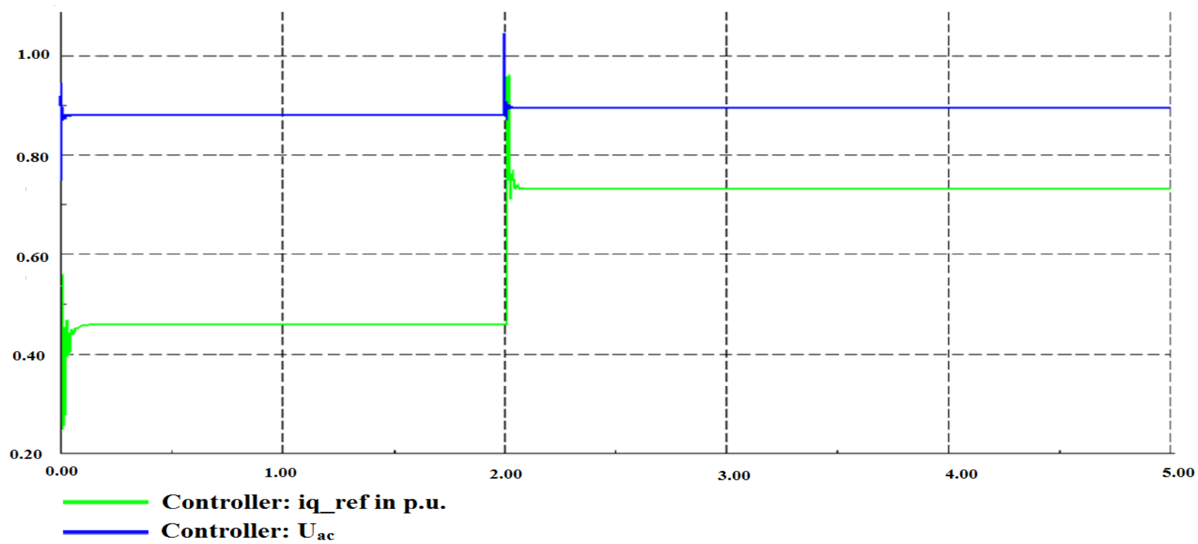

Figure 31 Voltage and reactive power fed at PCC with inverter delay = 10 ms; deadband = 0; droop = 20 (Watt/V)

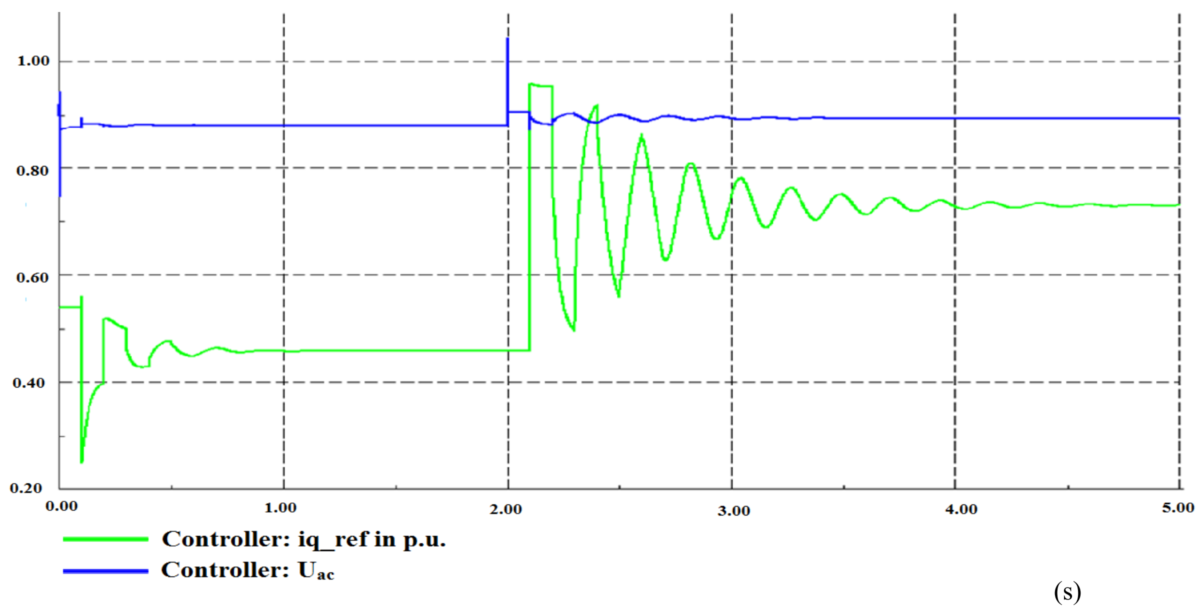

Figure 32 Voltage and reactive power fed at PCC with inverter delay = 100 ms; deadband = 0; droop = 20 (Watt/V)

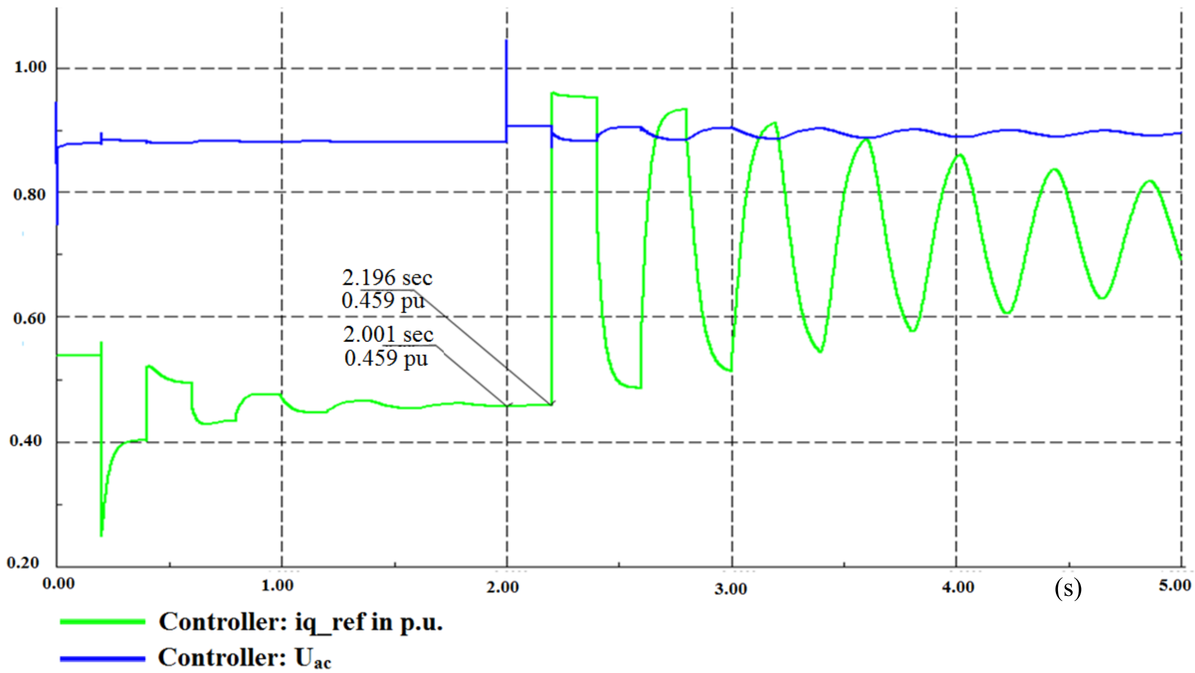

Figure 33 Voltage and reactive power fed at PCC with inverter delay = 200 ms; deadband = 0; droop = 20 (Watt/V)

The results for the reactive power injection at PCC are inferred to be dependent on the same parameters as that of the active power injection mentioned in section 5.3.1.1. It is clear that a voltage changes at PCC due to the sudden addition of loads. Injection of reactive power as a support to restore the voltage is seen to oscillate when a delay (in reactive power injection) is considered. The fluctuation at PCC increases with the inverter delay period, voltage droop value and affects the amplitude of the fluctuation that directly impacts the net stability of the LV grid. This effect can be mitigated through a few measures, such as designing an efficient inverter control to reduce the delay period, along with Demand side management. This would address a better control over the increasing PV penetration to electrical load time management. There are other measures in section 2.4 that might provide possible solutions to reduce this impact.

5.3.3 Voltage support for system under fault condition

This section is an extension to the analysis performed in 5.3.2. A fault condition with an additional PV inverter rated the same as the first are the inclusions made here. It is inferred that the oscillations due to delay increases in the presence of a fault. Through simulations, a single phase line to ground, a two phase and a three phase faults with different delay values are analyzed. A parameter event initiates a fault at 4 sec which is cleared within a period of 100 milli seconds. The impact it generates on the same system is shown in this section.

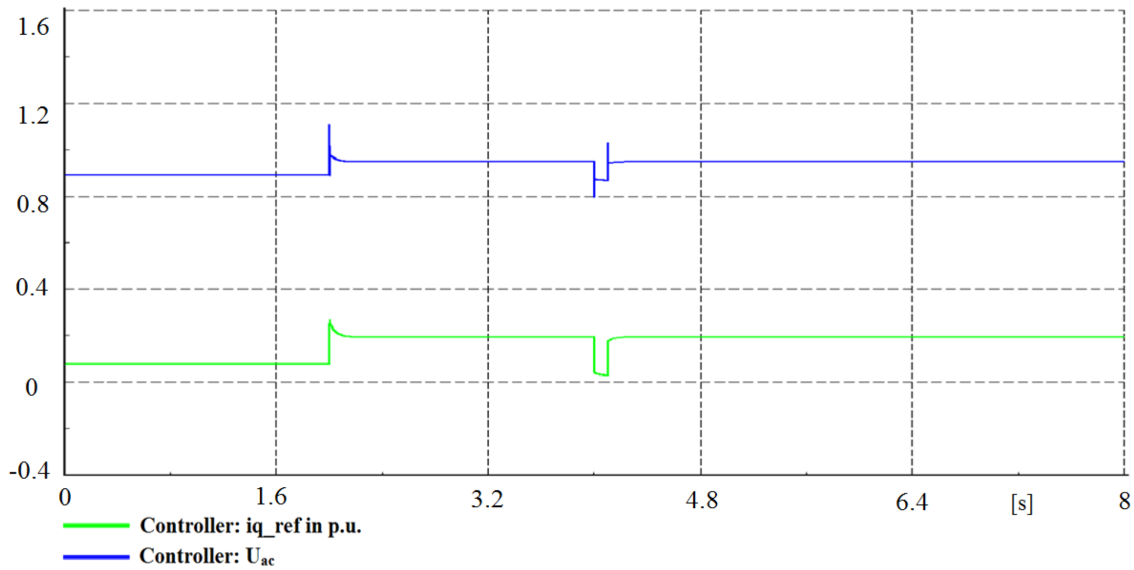

Figure 34 Single phase line to ground fault at t=4s clearance time 100 ms, 0 ms delay

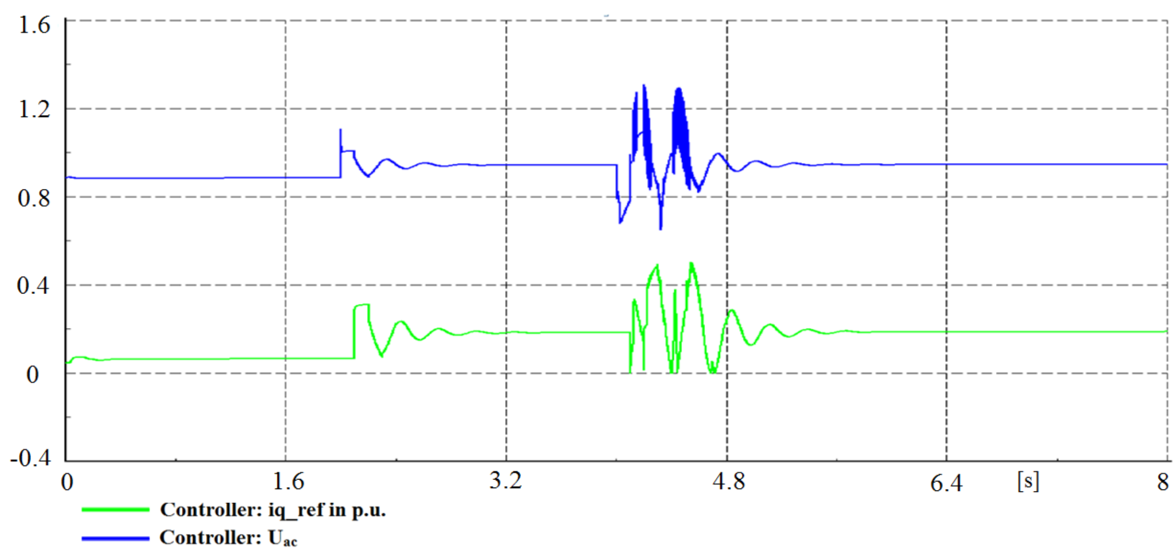

Figure 35 Single phase line to ground fault at 4s clearance time 100 ms, delay 100 ms

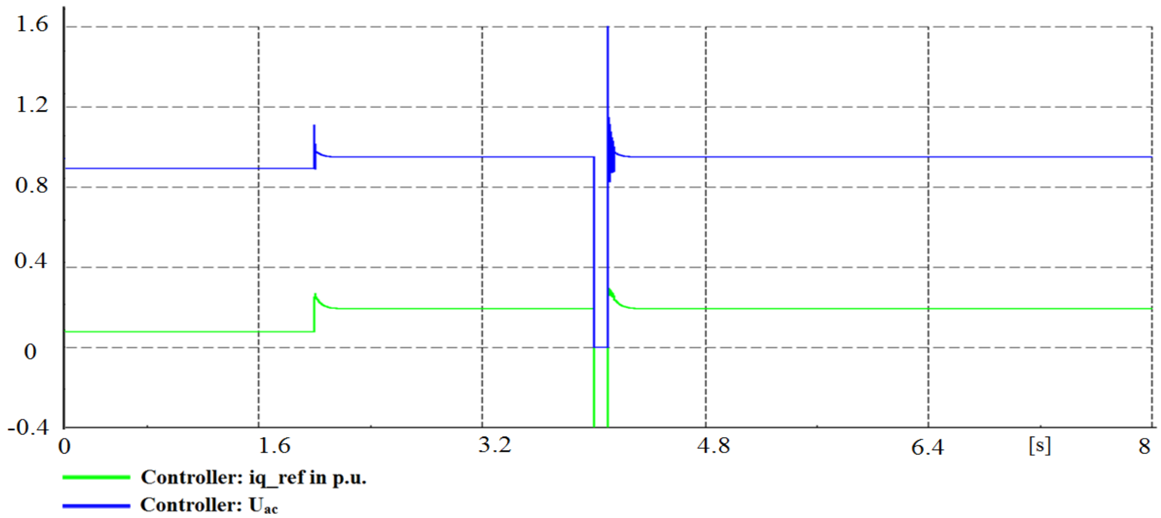

Figure 36 Three phase fault at t=4s with clearance time 100 ms, 0 ms delay

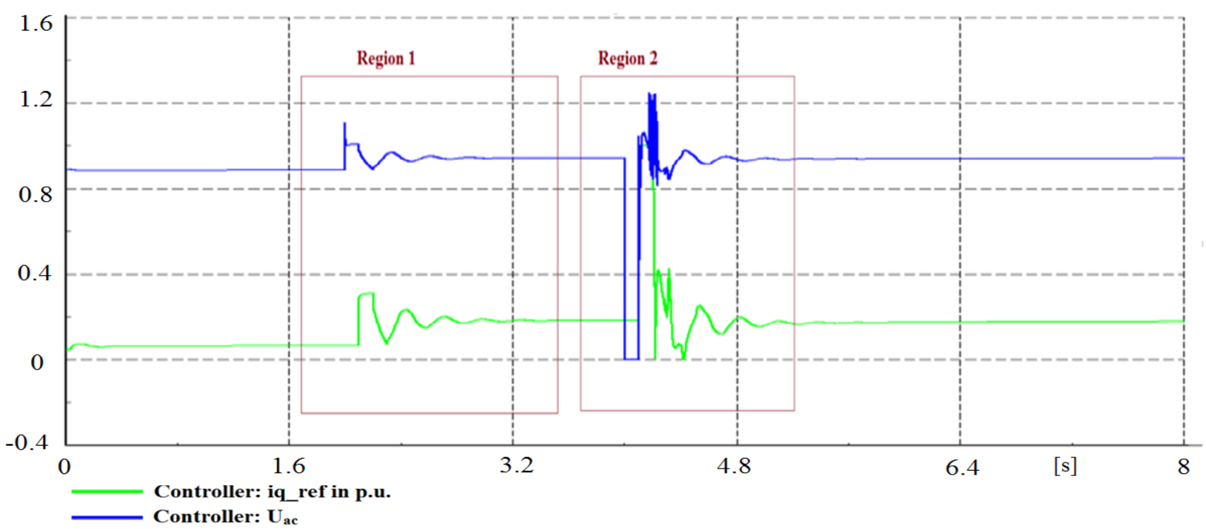

Figure 37 Three phase fault at t=4s with clearance time 100 ms with delay 100 ms

The impact due to a three phase fault along with an inverter feed-in delay has more deviation and spikes when compared to the region 1 (absence of a fault). The system as such can restore itself to a steady state condition in case of a single phase or three phase fault, but with some oscillations in presence of a delay in inverter fed power. This might lead the system to an unstable state for a certain period of time. Refer appendix section v for simulations performed for different faults with different delay times for the simple two bus model.

Fault type	Delay period [ms]		Voltage level in the LV bus				Reactive Power (Inverter)		Active Power (Inverter)	
			Inverter 1		Inverter 2		1	2	1	2
			[p.u.]	kV	[p.u.]	kV	[p.u.]	[p.u.]	[p.u.]	[p.u.]
3∅ to ground	100	100	1.059	0.245	1.056	0.244	-0.06	-0.25	0.26	0.17
	200	100	0.784	0.181	0.657	0.152	-0.09	-0.3	0.35	0.18
	10	100	0.938	0.217	1.030	0.238	-0.09	-0.35	0.38	0.45
2∅ to ground	100	200	0.938	0.217	1.031	0.238	-0.09	-0.35	0.38	0.45
	200	200	0.951	0.22	0.854	0.197	-0.05	-0.3	0.28	0.12
	10	200	0.939	0.217	1.033	0.238	-0.09	-0.35	0.38	0.45
3∅ to ground	100	10	0.998	0.230	1.091	0.252	-0.05	-0.36	0.34	0.45
	200	10	0.939	0.217	1.031	0.238	-0.09	-0.35	0.38	0.45
	10	10	0.942	0.218	1.037	0.239	-0.09	-0.34	0.38	0.45

Fault type	Delay period [ms]		Line connected to the external grid		
			P (MW)	Q(MVAR)	Overloading (%)
1∅ to ground	100	100	0.37	-0.34	189.37 %
	200	100	0.31	-0.51	303.28 %
	10	100	0.59	-0.56	347.67 %
2∅ to ground	100	200	0.59	-0.56	347.67 %
	200	200	0.29	-0.40	208.61 %
	10	200	0.59	-0.56	347.33 %
3∅ to ground	100	10	0.59	-0.56	346.68 %
	200	10	0.59	-0.56	347.51%
	10	10	0.57	-0-52	310.72

Table 5 Aggregated results under fault conditions for the test case

5.3.4 Quantitative analysis of simulation results

For the simulated results in section 5.3.2 the oscillations are analyzed following a switch of the loads by a fitting procedure. In order to get a quantitative estimate of the frequency f, amplitude A, damping time τ , we fit the oscillations to an exponential decaying oscillating function with t_o as the starting time of oscillation and B as the offset value. The fit function is,

$$A(t) = Ae^{-(t-t_0)/\tau} \cos(\omega(t - t_0)) + B \qquad 5.\ 1$$

The result of the fitting procedure shown in Table 6 summarizes the fit parameters obtained for simulations with different delay times. Figure 38 is the fit result of Figure 32 in MS Excel.

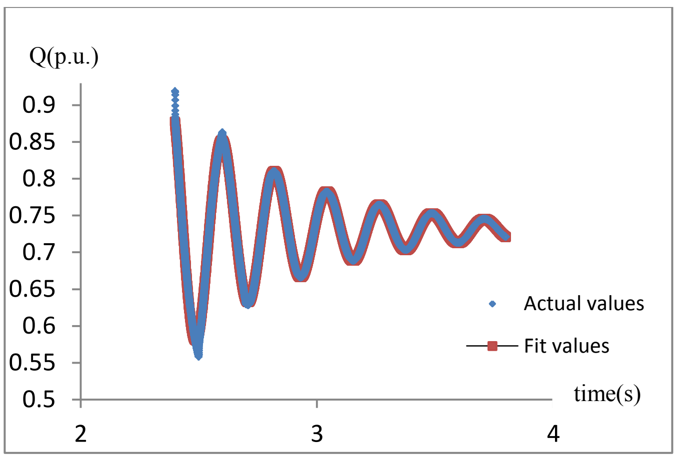

Figure 38 The underdamped oscillating curve from Figure 32 is plotted after Curve fitting

Fitting Variables	Values Obtained after fitting				
Delay time (ms)	**10**	**100**	**150**	**200**	**250**
A	0.185	0.184	0.185	0.24	0.355
ζ (tau)	0.01	0.524	0.01	2.131	3.139
ω	0.064	0.035	0.053	0.067	0.008
B	0.73148	0.73021	0.73081	0.73	0.73019

Table 6 Fitting Variables tabulated for a few delay periods

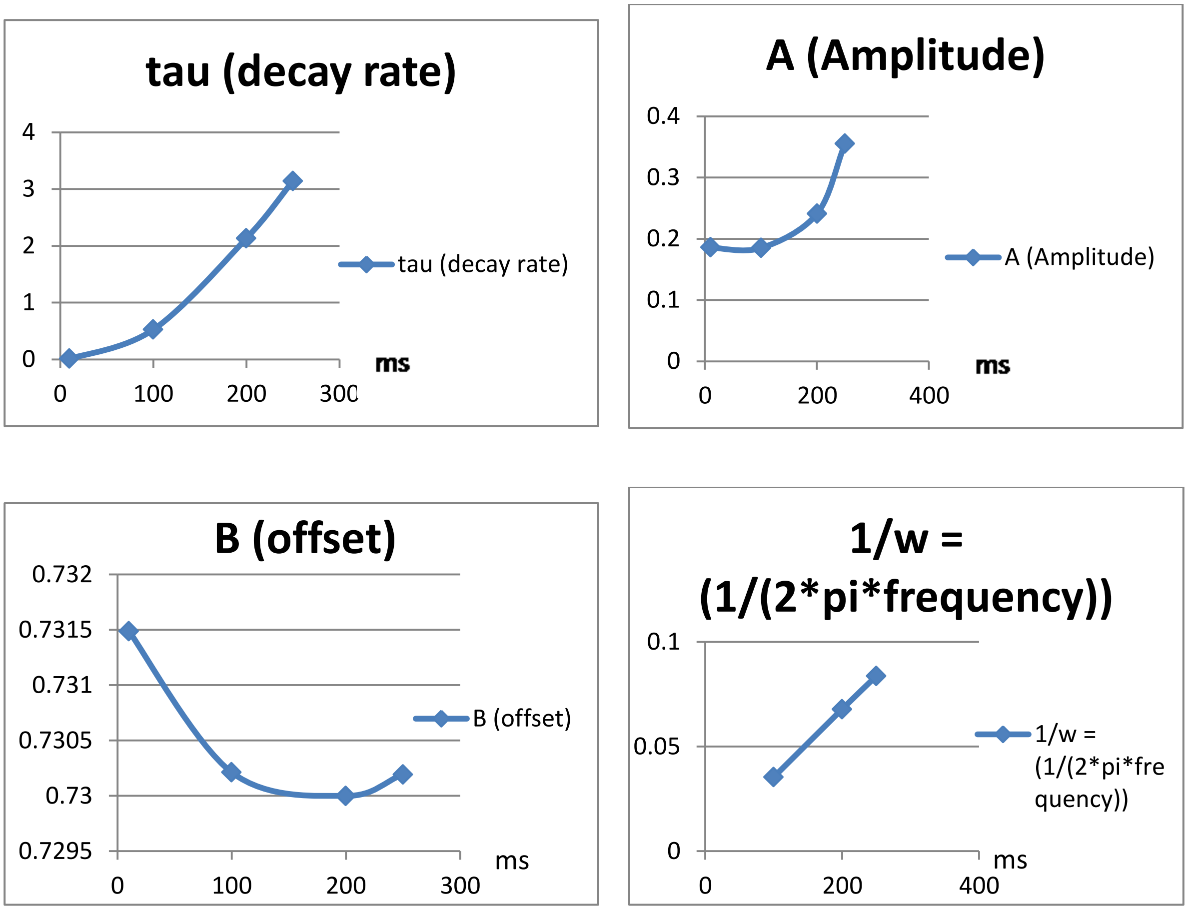

Figure 39 The values summarized in Table 6 are plotted with reference to delay time

For the set of simulations performed for voltage support with different inverter feed in delay times, their oscillation are fitted and analyzed as shown in Figure 39. τ is the decay time calculated to find the envelope of the underdamped oscillation. It is seen that for an increase in the delay time, the fit parameters τ , A and f are seen to be increasing. The offset value B decreases with an increase in the delay time.

5.4 Developing a Scenario for grid tied Photovoltaic and Electric Vehicles

This section describes a set of scenarios that may be considered on a test case based on a common pattern referred from literature, particularly the different EV charging strategies. The researchers have predefined a set of scenarios to highlight the same. In addition to this, the characteristics mentioned under section 2.2.2 may also be included. The scenarios compare uncontrolled and controlled or staggered charging patterns of EV [4][7][31][37][38]. One of the papers, Calero et al., [4] studies six different scenarios on an LV - PDG in the presence of both, controlled and uncontrolled EV charging patterns to find its grid impacts. The analysis was based on the power demand curve of houses and solar radiation curve.

On a common note, most of these papers contain a base scenario with constant loads, and DGs. A second scenario includes storage elements in addition to the base loads and DG. Third scenario is an extension to the second along with an additional predefined number of Electric vehicles per node (at the grid level). Three scenarios are combined in different forms in different papers. The idea of these scenarios is to compare the controlled and uncontrolled EV charging pattern, influence of a PV and storage in the system. The comparative results of aggregated load i.e., uncontrolled EV load, during evening peak demand period is considered as an inefficient condition and hence most researchers support a control over the EV charging.

To relate the available research scenarios with our project interests, following infrastructures are suggested. The infrastructures include different elements in every single case. As an example, three building infrastructures and three grid infrastructures are suggested to better explain the EV and PV grid connection.

5.4.1 Scenario 1

Initially, a base setup for residential building can be considered that contains at least a single DC or AC charging station for EV combined with a standard (regular every day load) building load. To specify the scenario in depth, certain statistical and deterministic values for the EVs and charging stations (with and without co-ordinated charging) can be noted. This scenario can be simulated without considering PV and storage elements.

- Data For Electric Vehicle can include
    - EV distribution time (based on driving pattern, arrival and departure time).
    - Battery status of EV, charging time (based on SOC)
- The charging stations can be detailed with some deterministic values of
    - Number of stations and type of each station

- Energy profile for charging process
- Recovering time between charging two vehicles

- Other general characteristics that could to be considered are
  - Amount of energy available in each time interval must be determined.
  - Power quality requirements including voltage limits, power factor limits and a few others mentioned in sections 2.3 and 2.4.1 can be considered.
  - This also includes specification of boundary conditions while charging.

5.4.2 Scenario 2

This is an extension of the section 5.4.1 with an inclusion of storage facilities and electric loads that can be varied and controlled. The integration of storage with regular loads increases the ability of load shifting. Further, the variable electrical loads assisted through a demand side management can be altered based on the source availability with controlling. It is possible to impose lower and upper limits to the consumed energy with certain constraints. Additional constraints imposed on the storage devices and the variable consumers, requires the state of each piece of equipment to be equal at the initial and end of the considered time horizon. This scenario can be elaborated through deterministic values of the following constraints:

- For Storage, certain details like maximal storage capacity, maximal change of storage level per period, initial and final storage level will have to be specified.
- Details for consumer with variable demands will include maximal and minimal energy demand per period and energy level to be obtained after a certain number of periods.

5.4.3 Scenario 3

This infrastructure is an extension to the one specified in Subsection 5.4.2 with an inclusion of DER such as PV. If bidirectional chargers were installed, the ability of EVs to supply energy to the grid or building would have a similar effect as storage. In addition to the previous data,

- For DER, statistical data for the amount of power produced with an additional deterministic data for power quality of the produced energy will be helpful in a scenario study

6 Conclusion and Future work

This chapter summarizes the findings of the thesis. The EV and PV integration at PCC are in the early stages of realization, so there are several technical problems involved in such integration. Reconciliation is required as it is a natural coincidence between peak electricity demand and vehicles returning to a residence after a daily commute. This thesis discuses a few impacts at the PCC and a few measures to mitigate them with certain performance criteria.

This thesis focuses on one of the impacts due to an error in grid synchronization causing delay in the PV power injection. For analysis purpose, a generic model, complying with the German Grid codes is selected and examined in a simulative environment. The PV system is modeled by a static generator along with a control scheme for active power reduction and reactive power injection for voltage support. The EV is assumed as loads in this case.

The model is validated for power injection in accordance to the German GC for LV-PDG. For a stable operation of a power distribution network comprising DER (i.e., PV or wind) generators with voltage-supporting controllers (Q = Q (U)) and active power reduction controllers. The voltage and frequency measurement delay should be as small as possible. Given a certain amount of voltage or frequency measurement delay in a PV inverter, the PV inverter controller's droop gain must be chosen small enough in order to guarantee a stable operation. The range of suitable droop gain depends on the properties of the power distribution network to which the PV inverter is connected. Based on the findings presented in this thesis, the set of all suitable (i.e., stabilizing) PV controller parameters can be determined by means of numerical simulations. With an analysis over the present German GC, and the potential problems that might rise with a transportation delay, it will be an essential part for the grid codes to address the grid under such conditions. Some modifications for grid tied PV systems as stated by the GC can include additional details such as how and to what extent the effect of fluctuation can be mitigated in case of the latency as seen in this thesis.

The problem of voltage, frequency and power flow oscillations may become more severe and will be more difficult to treat if the power network topology is more complicated and if the power network contains more than one DER generator. Investigating such complicated setup will be the topic of future work. ie., the analysis may be extended to a simple micro grid as a case study, LV-PDG. The load flow and EV charging pattern is documented in this thesis. In the later stages, an analysis over EV, with Vehicle to Grid capability will be studied. Also, its integration with PV can be controlled in the presence of BESS (Battery Energy Management System). An addition of FACT devices in such a system could potentially influence to reduce the oscillations at PCC. Further, the stochastic nature of the load can be modeled (to analyze the EV charging pattern as an example) for a specific parking zone that is connected to the immediate MV or LV-PDG.

Bibliography

1. *G. Boyle, Renewable Energy – Power for a Sustainable Future, Oxford University Press, New York, USA, 2004*

2. *International Energy Agency Report. (2009). Technology road map: Electric and plug-in hybrid electric vehicles. [Online]: http://www.iea.org/papers/2009/EV_PHEV_Roadmap.pdf*

3. *BMU and German National Renewable Energy Action Plan 2010, picture accessed via https://www.dbadvisors.com/content/_media/DBCCA_German_FIT_for_PV_0511.pdf*

4. *H. Binder, "Power Control for Wind Turbines in Weak Grids: Concepts Development", Risø-R-118 (EN), 1999 http://www.risoe.dtu.dk/rispubl/VEA/veapdf/ris-r-1118.pdf*
5. *S. Grunau; F. W. Fuchs, "Effect of Wind energy Power injection into weak grids", Institute for Power Electronics and Electrical Drives, Christian-Alberchts-University, Kiel, Germany http://www.tf.uni-kiel.de/etit/LEA/dl-open/veroeff_2012/grunau_ewea_2012.pdf*

6. *C. Lagares, J.L.; R. Fernandez, J.M.; B. Payan, M.; R. Santos, J.M.; , "Synergy of photovoltaic generators and Electric Vehicles in a low voltage distribution grid," PowerTech, 2011 IEEE, vol., no., pp.1-6, 19-23*

7. *S. Shao; M. Pipattanasomporn; S. Rahman; , "Challenges of PHEV penetration to the residential distribution network," Power & Energy Society General Meeting, 2009. PES '09. IEEE , vol., no., pp.1-8, July 2009*

8. *US Department of Energy, Energy efficiency and renewable energy, http://www.fueleconomy.gov/feg/evtech.shtml*

9. *K. Yunus; H.Z. De La Parra; M. Reza; , "Distribution grid impact of Plug-In Electric Vehicles charging at fast charging stations using stochastic charging model," Power Electronics and Applications (EPE 2011), Proceedings of the 2011-14th European Conference on , vol., no., pp.1-11, Sept. 1 2011*

10. *The Federal Energy Regulatory Commission Staff. (2010, June 17th). National Action Plan on Demand Response*: *www.ferc.gov/legal/staff-reports/06-17-10-demand-response.pdf.*

11. *BS EN 50160:2000 British Standard, as discussed in http://www.energieverbraucher.de/files_db/dl_mg_1219066789.pdf*

12. *WP 1 task 1.6 Deliverable D1.4, "Learning from EV field tests", MERGE, 7th September 2011*

13. *WP 1 task 3 Deliverable D1.2, "Extend concepts of mg by identifying several EV smart control approaches to be embedded in the smart grid concept to manage EV individually or in clusters", Mobile Energy Resources in Grids of Electricity (MERGE), June 2010.*

14. *R.A. Verzijlbergh; Z. Lukszo; J.G. Slootweg; M.D. Ilic; , "The impact of controlled electric vehicle charging on residential low voltage networks," Networking, Sensing and Control (ICNSC), 2011 IEEE International Conference on , vol., no., pp.14-19, 11-13* http://ieeexplore.ieee.org/stamp/stamp.jsp?tp=&arnumber=5874933&isnumber=5874867

15. *Transportation electrification – A technology overview - 2011 report EPRI, p. 5-10 table 5-2* http://www.smartgridinformation.info/pdf/4525_doc_1.pdf

16. *M. Braun; , "Reactive power supply by distributed generators," Power and Energy Society General Meeting - Conversion and Delivery of Electrical Energy in the 21st Century, 2008 IEEE , vol., no., pp.1-8, 20-24 July 2008* http://ieeexplore.ieee.org/stamp/stamp.jsp?tp=&arnumber=4596266&isnumber=4595968

17. *I. Waseem, "Impacts of distributed generation on the residential distribution network operation", Master thesis, Virginia Polytechnic Institute and State University, Dec 2008*

18. *C.L.T. Borges; D.M. Falcao, "Impact of distributed generation allocation and sizing on reliability, losses and voltage profile," Power Tech Conference Proceedings, 2003 IEEE Bologna , vol.2, no., pp. 5 pp. Vol.2-, 23-26 June 2003.*

19. *"IEEE Trial-Use Guide for Electric Power Distribution Reliability Indices," IEEE Std 1366-1998 , vol., no., pp.i, 1999* http://ieeexplore.ieee.org/stamp/stamp.jsp?tp=&arnumber=769684&isnumber=16680

20. *C.A. Warren; R. Ammon; G. Welch, "A survey of distribution reliability measurement practices in the US," Power Delivery, IEEE Transactions on , vol.14, no.1, pp.250-257, Jan 1999*

21. *S. Duvall, "Plug-In Hybrid Electric Vehicles Technology Challenge". Presentation at the U.S. DOE Plug-In Hybrid Discussion Meeting. Electric Power Research Institute, May'06*

22. *S. W. Hadley and A. Tsvetkova. Oak Ridge National Laboratory. (ORNL - 2008, January)." Potential Impacts of Plug-in Hybrid Electric Vehicles on Regional Power Generation",* http://ornl.org/info/ornlreview/v41_1_08/regional_phev_analysis.pdf.

23. *M. Kintner-Meyer, K. Schneider and R. Pratt. Pacific Northwest National Laboratory. (2007, December) Impacts Assessment of Plug-in Hybrid Vehicles on Electric Utilities and Regional U.S. Power Grids Part1: Technical Analysis.* www.ferc.gov/about/com-mem/wellinghoff/5-24-07-technical-analy-wellinghoff.pdf.

24. *K. Clement, "Impact of Plug-in Hybrid Electric Vehicles on the Electricity System", Doctoral thesis, Katholieke Universiteit Leuven, Belgium* *https://lirias.kuleuven.be/bitstream/123456789/275627/1/K*

25. *S. Shao, "An approach to demand response for alleviating power system stress conditions due to electric vehicle penetration", Doctoral thesis, Virginia Polytechnic Institute and State University, Oct 2011.*

26. *E. Veldman; M. Gibescu; J.G. Slootweg; W.L. Kling; , "Technical benefits of distributed storage and load management in distribution grids," PowerTech, 2009 IEEE Bucharest , vol., no., pp.1-8, June 28 2009-July 2 2009*

27. *E. Veldman; , "Unlocking the hidden potential of electricity distribution grids," Electricity Distribution - Part 2, 2009. CIRED 2009. The 20th International Conference and Exhibition on , vol., no., pp.1-16, 8-11 June 2009*, *http://ieeexplore.ieee.org/stamp/stamp.jsp?tp=&arnumber=5371361&isnumber=5371103*

28. *P. Esslinger; R. Witzmann; , "Increasing grid transmission capacity and power quality by a new solar inverter concept and inbuilt data communication," Innovative Smart Grid Technologies Conference Europe (ISGT Europe), 2010 IEEE PES , vol., no., pp.1-8, 11-13 Oct. 2010,* *Online: http://ieeexplore.ieee.org/stamp/stamp.jsp?tp=&arnumber=5638867&isnumber=5638851*

29. *T. Gonen, "Electric Power Distribution System Engineering," New York: McGraw-Hill, 1985.*

30. *WP 2 task 2.2 Deliverable D2.2, "Adaptation and Enhancement of existing simulation platforms)", Mobile Energy Resources in Grids of Electricity (MERGE), 15th Feb 2011.*

31. *J. R. Pillai, "Electric Vehicle based battery storages for large scale wind power integration in Denmark", Doctoral thesis, Aalborg University, Dec 2010.*

32. *De Kock, Jan; Strauss, Cobus (2004). Practical Power Distribution for Industry (pp. 74-75)*

33. *Intelligent dump load for stand-alone smart grids from SM- Sunny Island; Online: http://files.sma.de/dl/4439/SL6000-DEN102310.pdf*

34. *E. Troester, "New German grid codes for connecting PV systems to the Medium Voltage Power Grid", 2nd International workshop on Concentrating Photovoltaic Power Plants: Optical Design, Production, Grid Connection, Darmstadt, Germany, March 2009*

35. *"Forecast Uptake and Economic Evaluation of Electric Vehicles in Victoria", Department of Transportation, State Government Victoria*

36. *IEEE Guide for Loading Mineral-Oil Immersed Power Transformers, IEEE Power Engineering Society, 2004.*

37. *K. Clement; E. Haesen; J. Driesen; "Coordinated charging of multiple plug-in hybrid electric vehicles in residential distribution grids," Power Systems Conference and Exposition, 2009. PSCE '09. IEEE/PES , vol., no., pp.1-7, 15-18*

38. *A. Salvador; T.C. Green; N. Shah; , "Effects of optimised plug-in hybrid vehicle charging strategies on electric distribution network losses," T&D Conference and Exposition, 2010 IEEE PES , vol., no., pp.1-6, April 2010*

39. *I. J. Nagrath and D. P. Kothari, "Power System Engineering," Tata McGraw-Hill Publishing Company Limited, New Delhi,1994.*

40. *T. V. Cutsem and C. Vournas, Voltage Stability of Electric Power Systems, Springer LLC, New York, 2008.*

41. *B. H. Lee and K. Y. Lee, "Dynamic and static voltage stability enhancement of power systems," IEEE transactions on Power Systems, Vol. 8, No. 1, pp. 231 - 238, 1993.*

42. *"Voltage and frequency droop control in low voltage grids by distributed generators with inverter front-end" Online:* http://www.esat.kuleuven.be/electa/publications/fulltexts/pub_1610.pdf

43. *R. Teodorescu, M. Liserre, P. Rodriguez, Grid Converters for Photovoltaic and Wind Power Systems, Wiley, United Kingdom, 2011*

44. *"ENTSO-E Draft Requirements for Grid Connection Applicable to all Generators - 27 October 2011"and "Network and system rules of the German transmission system operators", Transmission Code 2007* http://www.vde.com/de/fnn/dokumente/documents/transmissioncode%202007_engl.pdf

45. *I. Theologitis, "Aspects of general photovoltaic model examined under the German grid code for medium voltage", 1st international workshop on integration of solar power into power system, Aarhus, Denmark 2011*

46. *M. Braun, T. Stetz, B. Reimann, B. Valov, G. Arnold (2009). Optimal Reactive Power Supply in Distribution Networks – Technological and Economic Assessment for PV-Systems. 24th European Photovoltaic Solar Energy Conference and Exhibition. Hamburg, 2009*

47. *Technical Guideline - Generating Plants Connected to the Medium-Voltage Network - Jun 2008, BDEW – pgs 14, 21.*

48. *H. Saadet, Power System Analysis, McGraw-Hill, 1999*

49. *R. Majumder; A. Ghosh; G. Ledwich; F. Zare; , "Angle droop versus frequency droop in a voltage source converter based autonomous microgrid," Power & Energy Society General*

Meeting, 2009. PES '09. IEEE , vol., no., pp.1-8, 26-30 July 2009
http://ieeexplore.ieee.org/stamp/stamp.jsp?tp=&arnumber=5275987&isnumber=5260217

50. *M. N. Marwali, M. Dai; A. Keyhani, "Robust stability analysis of voltage and current control for distributed generation systems" IEEE Trans. on Energy Conversion, Vol. 21, Issue-2, pp. 516-526, 2006.*

51. *M. Reza, D. Sudarmadi, F. A. Viawan, W. L. Kling, and L. Van Der Sluis, "Dynamic Stability of Power Systems with Power Electronic Interfaced DG," Power Systems Conference and Exposition, PSCE'06, pp. 1423-1428, 2006.*

52. *A. Ghosh, G. Ledwich,"High bandwidth voltage and current control design for voltage source converters", Australian Universities Power Engineering Conference, 2010, Canterbury, Christchurch, http://eprints.qut.edu.au/39327/1/c39327.pdf*

53. *Short Transmission lossy line http://www.amanogawa.com/archive/docs/C-tutorial.pdf*

54. *G. Villalva; J.R. Gazoli; E.R. Filho; , "Comprehensive Approach to Modeling and Simulation of Photovoltaic Arrays," Power Electronics, IEEE Transactions on , vol.24, no.5, pp.1198-1208, May 2009 http://ieeexplore.ieee.org/stamp/stamp.jsp?tp=&arnumber=4806084&isnumber=4815917*

55. *P. Kundur, "Vice-president, Power Engineering," in Power System Stability And Control, J Neal and G Mark, Eds. Palo Alto, California, USA: McGraw-Hill, 1994.*

56. *DIgSILENT Power Factory GMBH. user manual version 14*

57. *"Parking Study Supermarket Site Maclean NSW May 2011", Wakefield planning ITEM 13.125/11-1*

58. *M. Grünig, M. Witte, D. Marcellino, J. Selig, H. Van Essen, "An overview of Electric Vehicles on the market and in development" European Commission, Climate Action*

Appendix

i. Line characteristics under normal steady state conditions

System quantities	Parameter values	
	1-2 sequence	0 sequence
System frequency	50 Hz	50 Hz
Load (R_L)	260 kW	260 kW
Line Resistance (R_{Line})	0.1264 ohm	0.5057 ohm
Line Reactance (X_{Line})	0.06597 ohm	0.2638 ohm
Line Susceptanec (B_{Line})	336.1504 micro Siemens	184.7571 micro Siemens
Rated Line current	0.36 kA	0.36 kA

Table 7 General electric characteristics of line and load at steady state condition

ii. Parameters used in the DIgSILENT Photovoltaic model

DC Busbar and Capacitor		
Parameter	**Symbol**	**Value**
Capacity of the capacitor on DC busbar [s]	Capacity	0,0172
Initial DC voltage [V]	Udc0	700
Nominal DC voltage [kV]	UdcN	1
Rated Power [MW]	Pnen	0,5

Table 8 Parameters used in DC Busbar and Capacitor

PV Array slot		
Parameter	**Symbol**	**Value**
Open circuit voltage of module in STC [V]	UI0	43,8
MPP voltage of module in STC [V]	Umpp0	35
MPP current of module in STC [A]	Impp0	4,58
Short-circuit current of module in STC [A]	Ik0	5
Temperature correction factor (voltage) [1/K]	au x	-0,0039
Temperature correction factor (current) [1/K]	ai	0,0004
Number of modules connected in series [-]	nSerialModules	20
Number of modules connected in parallel [-]	nParallelModules	140
Time constant of module [s]	Tr	0

Table 9 Parameters used in PV array slot

Active Power Reduction		
Parameter	**Symbol**	**Value**
Start of active power reduction [Hz]	fUp	50,2
End of active power reduction [Hz]	fLow	50,05
Gradient of active power reduction [%/Hz]	gradient	40
PT1-Filter Time Constant [s]	Tfilter	0,01

Table 10 Parameters used in Active power reduction slot

Controller		
Parameter	**Symbol**	**Value**
Gain of the active power PI controller [-]	Kp	0,005
Integration time constant of the active power PI controller [s]	Tip	0,03
Measurement delay [s]	Tr	0,001
Time delay MPP-Tracking [s]	Tmpp	5
Deadband for AC voltage support [p.u.]	deadband	0,1
Droop static for AC voltage support [-]	droop	1
i_EEG = 0 according to TC2007; i_EEG = 1 according SDLWindV [-]	i_EEG	1
Minimum active current limit [p.u.]	id_min	0
Minimum allowed DC - voltage [V]	U_min	333
Minimum reactive current limit [p.u.]	iq_min	-1
Maximum active current [p.u.]	id_max	1
Maximum reactive current [p.u.]	iq_max	1
Maximum allowed absolute current [p.u.]	maxAbsCur	1
Maximum absolute reactive current in normal operation [p.u.]	maxIq	1

Table 11 Parameters used in Main Controller slot

Slot Name	Description	Type
Static Generator	Representation of the inverter in the single line diagram	*.ElmGenstat
Photovoltaic Model	DSL model of the PV cell	*.ElmDsl
DC Busbar & Capacitor Model	DSL representation of the DC system (in not included in the static generator model)	*.ElmDsl
Controller	Control unit, regulates the DC voltage and the reactive power	*.ElmDsl
Power Measurement	Power measurement device, needed for control feedback	*.StaPqmea
AC Voltage	AC voltage measurement device, needed for fault detection	*.StaVmea
Phase Measurement	PLL, needed for voltage angle measurement, input to the static generator	*.ElmPhi__pll
Active Power Reduction	DSL model with power reduction logic in case of over frequency	*.ElmDsl
Slow Frequency Measurement	PLL, with slow settings for measuring the frequency	*.ElmPhi_pll
Solar Radiation	Slot for radiation model (filled with inactive ramp model in the template)	*.ElmDsl
Temperature	Slot for temperature model (filled with inactive ramp model in the template)	*.ElmDsl

Table 12Frame Description for slots used for PV grid tied model in Power Factory

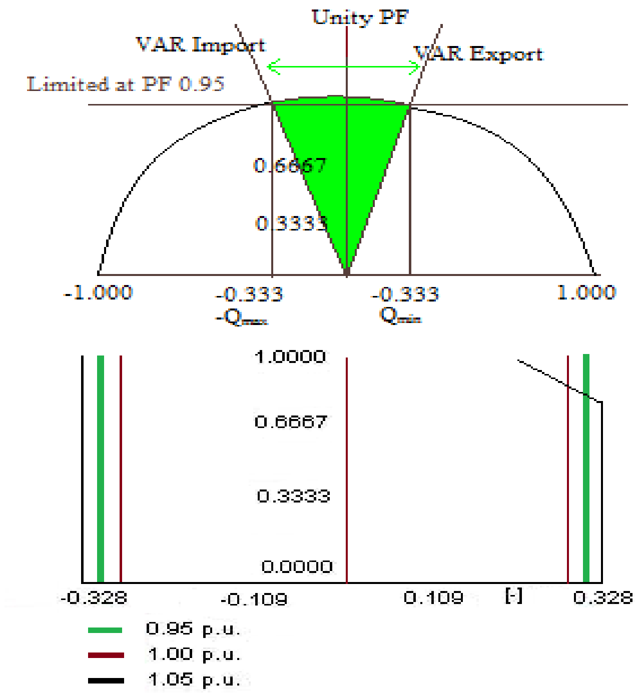

Figure 40 Capability curve that determines the amount of reactive power injection [56].

	0.00 p.u.	0.10 p.u.	0.50 p.u.	0.80 p.u.	1.00 p.u.
0.95 p.u.	0.296	0.296	0.296	0.296	0.296
1.00 p.u.	0.312	0.312	0.312	0.312	0.312
1.05 p.u.	0.328	0.328	0.328	0.328	0.328

Table 13 Matrix for Qmax (p.u.)

	0.00 p.u.	0.10 p.u.	0.50 p.u.	0.80 p.u.	1.00 p.u.
0.95 p.u.	-0.296	-0.296	-0.296	-0.296	-0.296
1.00 p.u.	-0.312	-0.312	-0.312	-0.312	-0.312
1.05 p.u.	-0.328	-0.328	-0.328	-0.328	-0.328

Table 14 Matrix for Qmin(p.u.)

iii. DIgSILENT code for Photovoltaic grid tie model

```
inc(yneu)=1
inc(yalt)=1
yneu=lim(select(yi<=fUp,1,1-gradient/100*(yi-fUp)),0,1)
yalt=delay(min(yo,yneu),0.01)
yo=select(yi<fLow,yneu,yalt)
```

Figure 41 DSL code for active power reduction block

```
!limitation of the current phasor
inc(det)= maxAbsCur*maxAbsCur-iqin*iqin
det= abs(lim(maxAbsCur*maxAbsCur-iqin*iqin,0,maxAbsCur*maxAbsCur))
delta=sqrt(det)

!in our case the i_frt is abs(yi)>deadband (boolean)
i_frt=picdro(abs(duac)>deadband,0,select(i_EEG,0,0.5))
idout=select(i_frt,lim(idin,-maxAbsCur+abs(iqin),maxAbsCur-abs(iqin)),
lim(idin,-maxAbsCur,maxAbsCur))
iqout=select(i_frt,lim(iqin,-maxAbsCur,maxAbsCur),
lim(iqin,-min(delta,maxIq),min(delta,maxIq)))
```

Figure 42 DSL code in current limiter block

```
inc(xtracker)=yo1
inc(yo1)=K*yi+limstate(x,yo_min,yo_max)
inc(yo2)=pred*yo1
x.=select({pred<1 .and. yi>=0}, 0, select(T>0,K*yi/T,0))
xtracker.=select(pred<1,0,(yo1-xtracker)/0.1)
yo1=select(T>0,lim(K*yi+limstate(x,yo_min,yo_max),yo_min,yo_max),K*yi)
yo2=lim(xtracker*pred,yo_min,yo_max)

yo=select(pred<1,min(yo1,yo2),yo1)
limits(T)=(0,]
```

Figure 43 DSL code in the PI controller Block

```
inc(i0)=iq
inc(iq0)=iq
inc(iq1)=iq
!according Transmission Code 2007
i_frt=picdro(abs(yi)>deadband,0,select(i_EEG,0,0.5))
!in our case the i_frt is abs(yi)>deadband (boolean)

!the following expression is not useful in our case
iq0=lim(select(i_frt,abs(yi)/yi*abs(yi)*droop+i0,i0),iq_min,iq_max)

!according SDLWindV
iq1=lim(select(i_frt,abs(yi)/yi*(abs(yi)-deadband)*droop+i0,i0),iq_min,iq_max)


!select output
iq=select(i_EEG,iq1,iq0)
```

Figure 44 DSL code in the Reactive power support block

```
!------------------------------------------!
!  Model of a Photovoltaic Module          !
!     - Current Voltage Characteristic     !
!     - Dependency of Solar Radiation,     !
!       valid for E >> 1 W/m²              !
!     - Dependency of Module Temperature   !
!------------------------------------------!

!vardef(Ul0)    = 'V';    'Open-circuit Voltage (STC)'
!vardef(Ik0)    = 'A';    'Short-ciruit Current (STC)'
!vardef(Umpp0)  = 'V';    'MPP Voltage (STC)'
!vardef(Impp0)  = 'A';    'MPP Current (STC)'
!vardef(au)     = '1/K'; 'Temperature correction factor (voltage)'
!vardef(ai)     = '1/K'; 'Temperature correction factor (current)'

!vardef(Ul)     = 'V'; 'Open-circuit Voltage'
!vardef(Ik)     = 'A'; 'Short-ciruit Current'

!vardef(Umpp)   = 'V'; 'MPP Voltage'
!vardef(Impp)   = 'A'; 'MPP Current'
!vardef(Pmpp)   = 'W'; 'Power at MPP'

!vardef(U)      = 'V'; 'Voltage'
!vardef(I)      = 'A'; 'Current'
!vardef(P)      = 'W'; 'Power'
inc(E)=1000
! Constants / Konstanten
inc(lnEstc) = ln(1000)                        ! ln of E at STC
inc(ImppIk) = ln(1-Impp0/Ik0)
!----------------------------------
```

(CONT)

```
! Equations / Gleichungen
! Temperature Dependency:
tempCorrU = 1+au*(theta-25)                        ! Voltage Correction Factor
tempCorrI = 1+ai*(theta-25)                        ! Current Correction Factor
! Open-circuit voltage:
E_help  = max(E, 1.0)                              ! to avoid ln(0) in next equation
lnEquot = select(E>1.0, ln(E_help)/lnEstc, 0.0)    ! ln(E)/ln(1000W/m²), if E > 1W/m²
Ul = Ul0*lnEquot*tempCorrU                         ! Open-circuit voltage dependent from E and theta
! Short-circuit current:
!Ik = Ik0*E/1000*tempCorrI                         ! Short-circuit current dependent from E and theta
Ik = select(E>1, Ik0*E/1000*tempCorrI, 0.0)        ! Current generation only if E>1 (limitation of model)
! Maximum Power Point:
Umpp = Umpp0*lnEquot*tempCorrU                     ! MPP voltage dependent from E and theta
!Impp = Impp0*E/1000*tempCorrI                     ! MPP current dependent from E and theta
Impp = select(E>1, Impp0*E/1000*tempCorrI, 0.0)    ! Current generation only if E>1 (limitation of model)
Pmpp = Umpp * Impp
! Voltage of MPP (output signal)
Vmpp = Umpp
! Current:
! Approximation:
! Internal Variables:
c3 = 0.0
c4 = select(Ul>0, Umpp - Ul, 1.0)                  ! to avoid division by 0 in equation for c2
c2 = select(Ul>0, select(c4<0, ImppIk/c4, 0.0), 0.0)
c1 = min(max(c2*(U-Ul),-13),3)
! Current output (output signal)
I = max(Ik*(1-exp(c1)),0.0)
! Power:
P = U * I
! Limits / Grenzen
limits(Ul0)    = (0,]
limits(Umpp0)  = (0,]
limits(Impp0)  = (0,]
limits(Ik0)    = (0,]
limits(E)      = [0,]
```

Figure 45 DSL code PV array Module

iv. Fault ride through capability:

The Fault Ride-Through capability abbreviated as FRT is a part of the dynamic voltage support that covers Low Voltage Ride-Through (LVRT) and reactive current injection requirements. The grid tied PV system need to provide dynamic grid support as per German GC that has framed a specific standard to examine LVRT behaviour. For static generator (absence of synchronous generator) the GC specifications are mentioned in the Table 15. The tests performed in reference to the prescribed standards are pursued whose specifications are mentioned in for such a condition it is necessary to analyze the system capabilities under fault conditions (single phase line to ground & three phase fault). So, the test model is studied for its FRT capability in the presence and absence of a delay of 100 ms. (Delay is in the inverter power fed at PCC).

Test	Maximum allowed line to line voltage U/Un	Fault duration [ms]
1	≤ 0.05	≥ 150
2	0.2 – 0.25	≥ 550
3	0.45 – 0.55	≥ 950
4	0.7 – 0.8	≥ 1400

Table 15 German GC for testing fault ride through conditions

v. Simulations performed with different time delays under fault conditions

These simulations are an extension to the discussion in 5.3.3 for different set of fault and delay times. The system might become unstable for larger delays as seen in Figure 49.

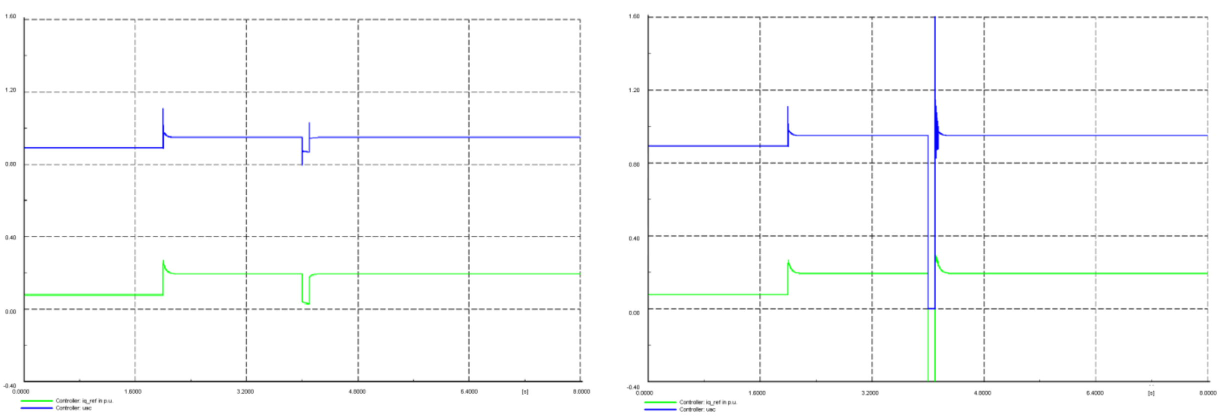

Figure 46 1 phase and 3 phase faults, Inverter 1 and 2 delay: 0 ms

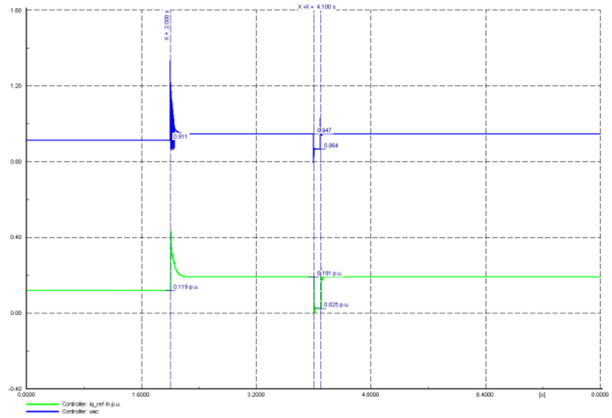

Figure 47 1 phase and 3 phase faults, Inverter 1 and 2 delay: 10 ms

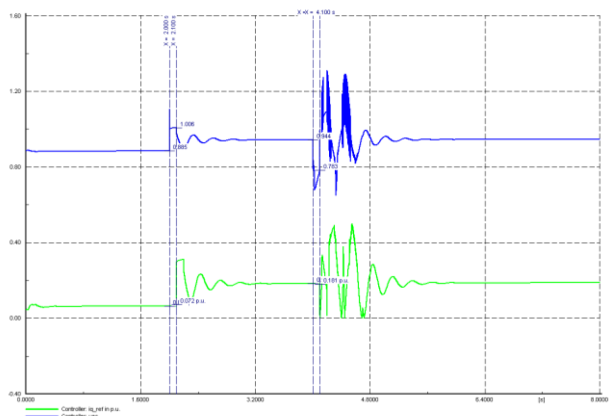

Figure 48 1 phase and 3 phase faults, Inverter 1 and 2 delay: 100 ms

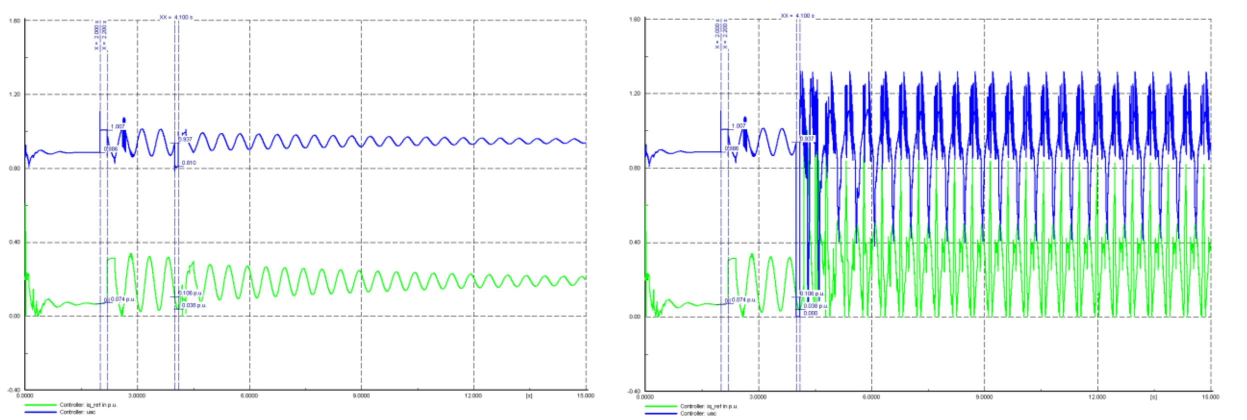

Figure 49 1 phase and 3 phase faults, Inverter 1 and 2 delay: 200 ms

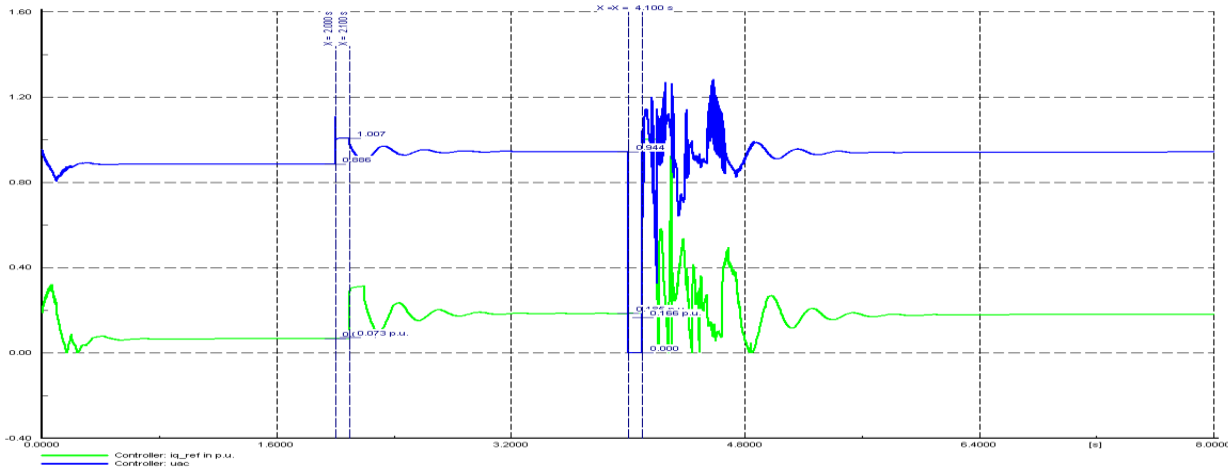

Figure 50 1 phase and 3 phase faults, Inverter 1: 100 ms and inverter 2 delay: 200 ms

vi. Transformer Overloading

The Figure 51 shows histograms of the future transformer loadings as discussed in [14]. The scenario without EV is considered as a base case. A regular 1% growth is shown as a line graph behind the histogram bars in the same case. Also, the amount of overloaded transformers in the different scenarios is displayed. The threshold value for a transformer to be overloaded is chosen to be 1.16 rather than one. This ensures that any instantaneous peak values are within the sustainability limits of the standard transformers compared to its nominal capacity. It should be noted that the value 1.16 is based upon historical load profiles (where a peak was normally sustained for short times). We use the value of 1.16 both the cases here. The uncontrolled 10kW charging scenario shows the largest amount of overloaded transformers: roughly 50%. Compared with the controlled charging scenario (21% overloading), which is a significant increase.

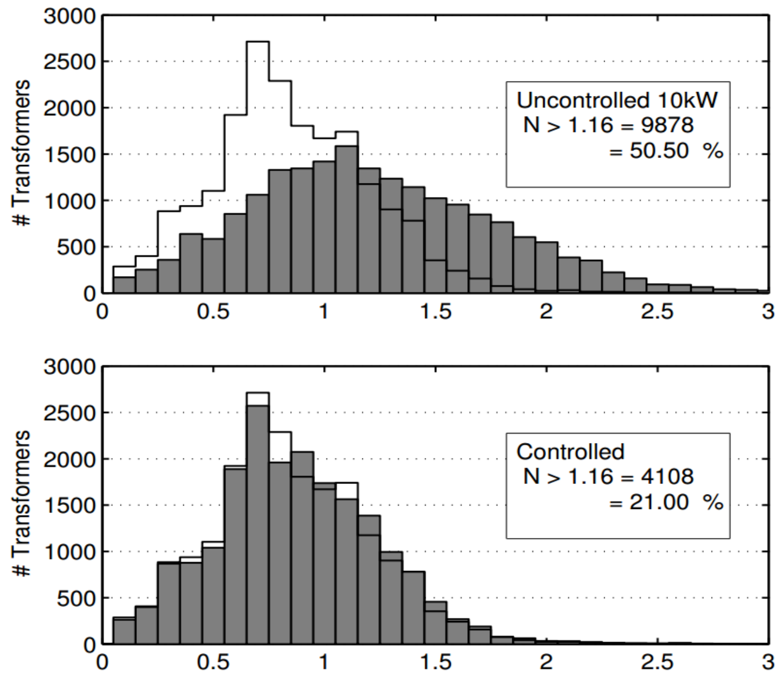

Figure 51 Loading distribution of a transformer considering 75% of households with EV